Role of breast regression protein 39 (BRP-39)/chitinase 3-like-1 in Th2 and IL-13–induced tissue responses and apoptosis

Chun Geun Lee,[1] Dominik Hartl,[1] Gap Ryol Lee,[2] Barbara Koller,[1] Hiroshi Matsuura,[1] Carla A. Da Silva,[1] Myung Hyun Sohn,[1] Lauren Cohn,[1] Robert J. Homer,[3] Alexander A. Kozhich,[4] Alison Humbles,[4] Jennifer Kearley,[4] Anthony Coyle,[4] Geoffrey Chupp,[1] Jennifer Reed,[4] Richard A. Flavell,[2] and Jack A. Elias[1]

[1]Section of Pulmonary and Critical Care Medicine, Department of Internal Medicine, [2]Section of Immunobiology, and [3]Department of Pathology, Yale University School of Medicine, New Haven, CT 06520
[4]MedImmune, Inc., Gaithersburg, MD 20878

Mouse breast regression protein 39 (BRP-39; Chi3l1) and its human homologue YKL-40 are chitinase-like proteins that lack chitinase activity. Although YKL-40 is expressed in exaggerated quantities and correlates with disease activity in asthma and many other disorders, the biological properties of BRP-39/YKL-40 have only been rudimentarily defined. We describe the generation and characterization of BRP-39$^{-/-}$ mice, YKL-40 transgenic mice, and mice that lack BRP-39 and produce YKL-40 only in their pulmonary epithelium. Studies of these mice demonstrated that BRP-39$^{-/-}$ animals have markedly diminished antigen-induced Th2 responses and that epithelial YKL-40 rescues the Th2 responses in these animals. The ability of interleukin13 to induce tissue inflammation and fibrosis was also markedly diminished in the absence of BRP-39. Mechanistic investigations demonstrated that BRP-39 and YKL-40 play an essential role in antigen sensitization and immunoglobulin E induction, stimulate dendritic cell accumulation and activation, and induce alternative macrophage activation. These proteins also inhibit inflammatory cell apoptosis/cell death while inhibiting Fas expression, activating protein kinase B/AKT, and inducing Faim 3. These studies establish novel regulatory roles for BRP-39/YKL-40 in the initiation and effector phases of Th2 inflammation and remodeling and suggest that these proteins are therapeutic targets in Th2- and macrophage-mediated disorders.

CORRESPONDENCE
Jack A. Elias:
Jack.elias@yale.edu

Abbreviations used: AHR, airways hyperresponsiveness; alum, aluminum hydroxide; AMCase, acidic mammalian chitinase; BAL, bronchoalveolar lavage; BRP-39, breast regression protein 39; CLP, chitinase-like protein; dox, doxycycline; Faim, Fas apoptosis-inhibiting molecule; HcGP, human cartilage glycoprotein; HDM, house dust mite; IHC, immunohistochemistry; mDC, myeloid DC; MMR, macrophage mannose receptor; mRNA, messenger RNA; pDC, plasmacytoid DC; PI, propidium iodide; PKB, protein kinase B; TARC, thymus- and activation-regulated chemokine; Tg, transgenic.

The evolutionarily conserved 18-glycosyl-hydrolase family contains true chitinases and molecules that lack chitinase activity (1–4). Much of the research in this area has focused on chitinases, like acidic mammalian chitinase (AMCase), that play critical roles in the life cycle of parasites (5, 6) and the pathogenesis of Th2 and antiparasite responses (3, 4, 7). However, the majority of the 18-glycosyl-hydrolase family members are chitinase-like proteins (CLPs), which, as a result of mutations in their highly conserved enzyme sites, do not contain chitinase activity. Breast regression protein 39 (BRP-39) and its human homologue YKL-40 (also called chitinase 3-like-1 and human cartilage glycoprotein [HcGP] 39) (8–10) are the prototypes of these enzymatically deficient CLPs. Surprisingly, their roles in biology have only been superficially addressed.

BRP-39 and YKL-40 are produced by a variety of cells including neutrophils, monocytes, macrophages, chondrocytes, synovial cells, smooth muscle cells, endothelial cells, and tumor cells (3, 8, 11). Increased levels of YKL-40 protein and/or messenger RNA (mRNA) have been noted in patients with a broad spectrum of pathologies including bacterial infections, rheumatoid arthritis, osteoarthritis, giant cell arteritis,

C.G. Lee and D. Hartl contributed equally to this paper.
G.R. Lee's present address is Dept. of Life Science, Sogang University, Seoul, Korea.

The Rockefeller University Press $30.00
J. Exp. Med. Vol. 206 No. 5 1149-1166
www.jem.org/cgi/doi/10.1084/jem.20081271

sarcoidosis, scleroderma, diabetes, atherosclerosis, inflammatory bowel disease, and solid malignancies (3, 8, 11–16). In many of these disorders, the levels of YKL-40 reflect the activity and natural history of the disease (2, 14–16). This is nicely illustrated in studies from our laboratory and from others, which have demonstrated that elevated levels of serum YKL-40 are seen in patients with asthma which correlate with the levels of lung tissue YKL-40 and disease severity (2). These studies also highlighted polymorphisms in chitinase 3-like-1 that correlated with the levels of circulating YKL-40, the presence of asthma, and compromised lung function (17). The potential importance of YKL-40 can also be seen in rheumatoid arthritis, coronary artery disease, solid cancers, and death in the elderly, where elevated serum YKL-40 levels correlate with the severity of joint involvement, the number of blocked coronary arteries, short disease-free intervals, and all-cause mortality, respectively (11, 14, 15, 18). As a result, YKL-40 is a prognostic biomarker and has been proposed to be a therapeutic target in conditions characterized by acute or chronic inflammation, extracellular matrix remodeling, fibrosis, and cancer (11, 18, 19). Because serum YKL-40 levels provide information that is different than that provided by established prognostic biomarkers, such as serum C-reactive protein, YKL-40 is believed to reflect different pathways in the pathogenesis of these disorders (11). However, our very limited understanding of the biology of BRP-39/YKL-40 makes it difficult to appreciate the true meaning of these disease-CLP associations and the ways that BRP-39 and YKL-40 contribute to normal biology and disease-relevant pathological responses. This is due, in part, to the fact that mice with null mutations of CLP and mice that overexpress CLP have not been generated, thereby limiting mouse modeling of these molecules. To address this deficiency and further define the biology of CLP, we generated and characterized mice with null mutations of BRP-39 (BRP-39$^{-/-}$), mice that overexpress YKL-40 in a lung-specific fashion, and mice that lack BRP-39 and produce YKL-40 only in their respiratory epithelium.

RESULTS

Regulation of BRP-39 by Th2 inflammation

To determine if BRP-39 is regulated by Th2 inflammation, we compared the expression of BRP-39 in lungs from control mice and mice that had been sensitized and challenged with the chitin-free antigen OVA. These studies demonstrated that the levels of BRP-39 mRNA and protein were significantly increased after OVA sensitization and challenge (Fig. 1, A–C). This was readily detected 24 h after aerosol OVA exposure and persisted at all time points that were assessed (Fig. 1 and not depicted). This induction was not seen in mice that received a saline aerosol after OVA-plus–aluminum hydroxide (alum) sensitization or an OVA aerosol after saline sensitization (unpublished data). In all cases, BRP-39 was induced predominantly in airway epithelial cells and alveolar macrophages (Fig. 1, D and E). This staining was appropriately specific because it was not present when the primary antibody was preincubated with BRP-39 peptide and when the primary antibody was not used in the evaluation (unpublished data). Interestingly, similar induction of BRP-39 was seen in lungs from mice sensitized and challenged with the chitin-containing antigen house dust mite (HDM) extract (Fig. 1 F and not depicted). Thus, BRP-39 is prominently induced during the course of chitin-free and chitin-containing antigen-induced Th2 inflammation.

Generation and preliminary characterization of BRP-39$^{-/-}$ mice

Homologous recombination was subsequently used to generate BRP-39$^{-/-}$ mice. The constructs that were used eliminated exons 1–6 and part of the BRP-39 promoter (Fig. S1). PCR, mRNA, and Western evaluations demonstrated the success of this approach (Fig. S1, B–D). These mice were bred for >10 generations onto a C57BL/6 or BALB/c background. At baseline, the BRP-39$^{-/-}$ mice were viable and fertile and were not able to be differentiated from the WT littermate controls based on size, physical appearance, rate of growth, or level of physical activity (unpublished data). In addition, autopsy, light microscopic examinations of skin and visceral organs, pulmonary compliance assessments, and H&E, trichrome, and elastin evaluations failed to reveal differences between WT and BRP-39$^{-/-}$ animals (unpublished data).

Role of BRP-39 in OVA-induced Th2 inflammation and physiological dysregulation

In WT mice, OVA-plus-alum sensitization and challenge caused a significant increase in tissue inflammation and bronchoalveolar lavage (BAL) total cell, eosinophil, and lymphocyte recovery (Fig. 2 A and Fig. S2). In these mice, increased numbers of CD4 Th2 cells and alternatively activated macrophages (M2 macrophages) were also seen (Fig. 2, B and C; Fig. S3; and not depicted). Exaggerated bronchospastic responses to methacholine challenge (airways hyperresponsiveness [AHR]; Fig. 2 D) and increased BAL Muc5ac and mucus metalasia were also noted (Fig. 2 E and not depicted). Similar responses were elicited in mice that were sensitized and challenged with the HDM extract (Fig. 2 F and data not depicted). In both experimental systems, each of these inductive events was at least partially BRP-39 dependent because null mutations of BRP-39 caused a significant decrease in each of these parameters (Fig. 2, A–F and Fig. S2). Importantly, these effects appeared to be at least partially Th2 specific because OVA-plus-complete-Freund's-adjuvant–induced Th1 inflammation and IFN-γ production were not similarly altered in BRP-39$^{-/-}$ mice (Fig. 2, G and H).

In WT mice, OVA-plus-alum sensitization and challenge caused significant increases in Th2 cytokine mRNA and protein (Fig. 2 I and not depicted). Comparable Th2 cytokine induction was not noted in mice with null mutations of BRP-39, with lung IL-13 and IL-4 being decreased by ≥80% (Fig. 2 I and not depicted). When viewed in combination, these studies demonstrate that BRP-39 plays a critical role in Th2 inflammation, physiological dysregulation, mucus metaplasia, and Th2 cytokine elaboration. They also demonstrate that BRP-39 plays a similar role in chitin-free and chitin-containing antigen-induced responses.

Role of BRP-39 in antigen sensitization and IgE induction

To begin to assess the mechanisms that underlie the defective Th2 responses in BRP-39$^{-/-}$ mice, studies were undertaken to determine if BRP-39 played a role in OVA-induced allergen sensitization. In these experiments, WT and BRP-39$^{-/-}$ mice received i.p. OVA plus alum. They were then boosted with antigen and antigen-induced splenocyte proliferation and the levels of antigen-specific IgE were assessed. In WT mice, sensitization resulted in readily appreciable antigen-induced splenocyte proliferation and increases in the levels of antigen-specific IgE (Fig. 3, A and B). Each of these responses was at least partially BRP-39 dependent because null mutations of BRP-39 significantly decreased each of these parameters (Fig. 3, A and B). In combination, these studies demonstrate that BRP-39 plays a critical role in antigen-induced sensitization and IgE induction.

BRP-39 regulation of pulmonary DCs

To further define the defects in antigen sensitization that were noted, we next compared the myeloid DC (mDC) and plasmacytoid DC (pDC) in lungs from WT and BRP-39$^{-/-}$ mice. In these experiments, the numbers of mDC and pDC were increased in lungs from WT mice that had been sensitized and challenged with OVA (Fig. 3, C and D). The mDC also

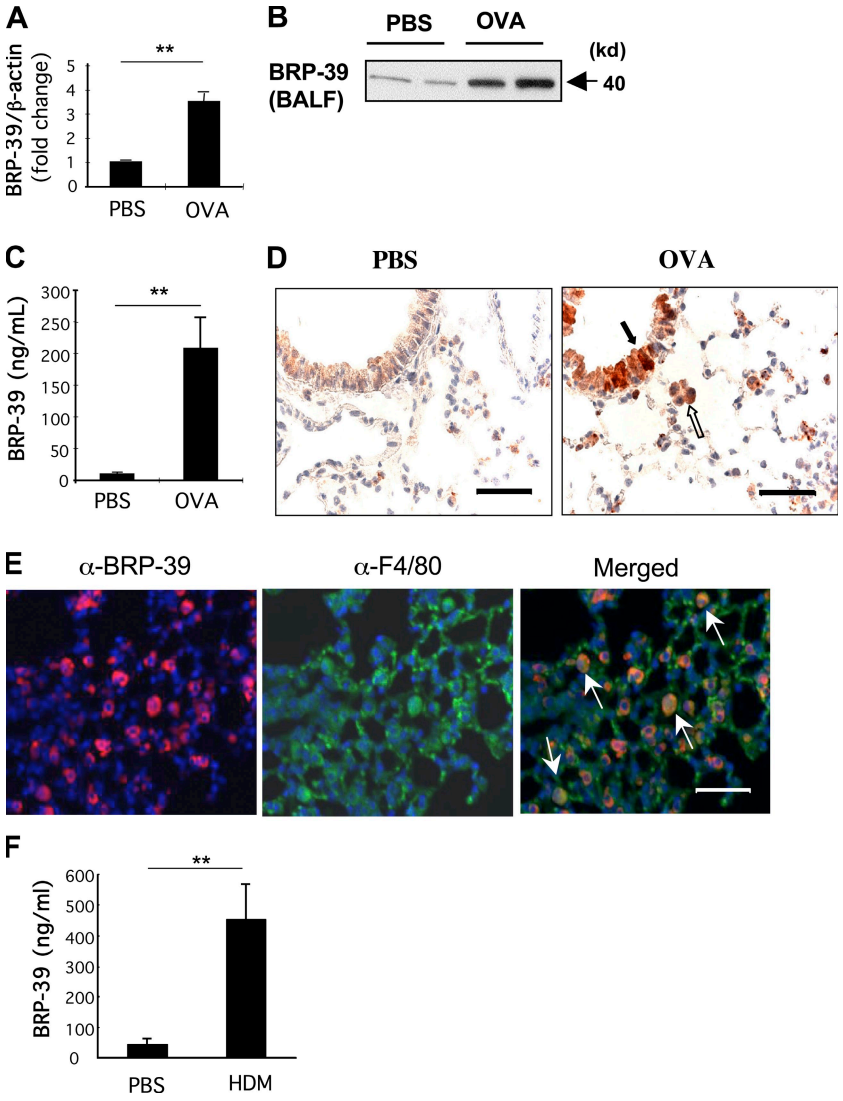

Figure 1. Regulation of BRP-39 during antigen-induced Th2 inflammation. (A–F) WT BALB/c mice were sensitized with OVA plus alum and challenged with PBS or OVA (A–E) or sensitized with HDM antigen plus alum and challenged with PBS or HDM (F). (A) The levels of BRP-39 mRNA were evaluated by real time RT-PCR. (B and C) BRP-39 accumulation was assessed via Western analysis (B) and ELISA (C) using lung lysate and BAL fluid, respectively. (D) Immunohistochemistry (IHC) was also used to localize the BRP-39 (solid arrow, airway epithelial cell; open arrow, alveolar macrophage). (E) Double-label IHC using BRP-39 and F4/80 antibodies, localized BRP-39, and F4/80-positive macrophages (white arrows, double^{+} cells). (F) The levels of BRP-39 in BAL fluids from PBS- or HDM-challenged mice, assessed by ELISA. Values in A, C, and F are the mean ± SEM of evaluations in a minimum of five animals and are representative of two separate evaluations. B, D, and E are illustrative of a minimum of three separate experiments. **, $P < 0.01$. Bars, 25 µm.

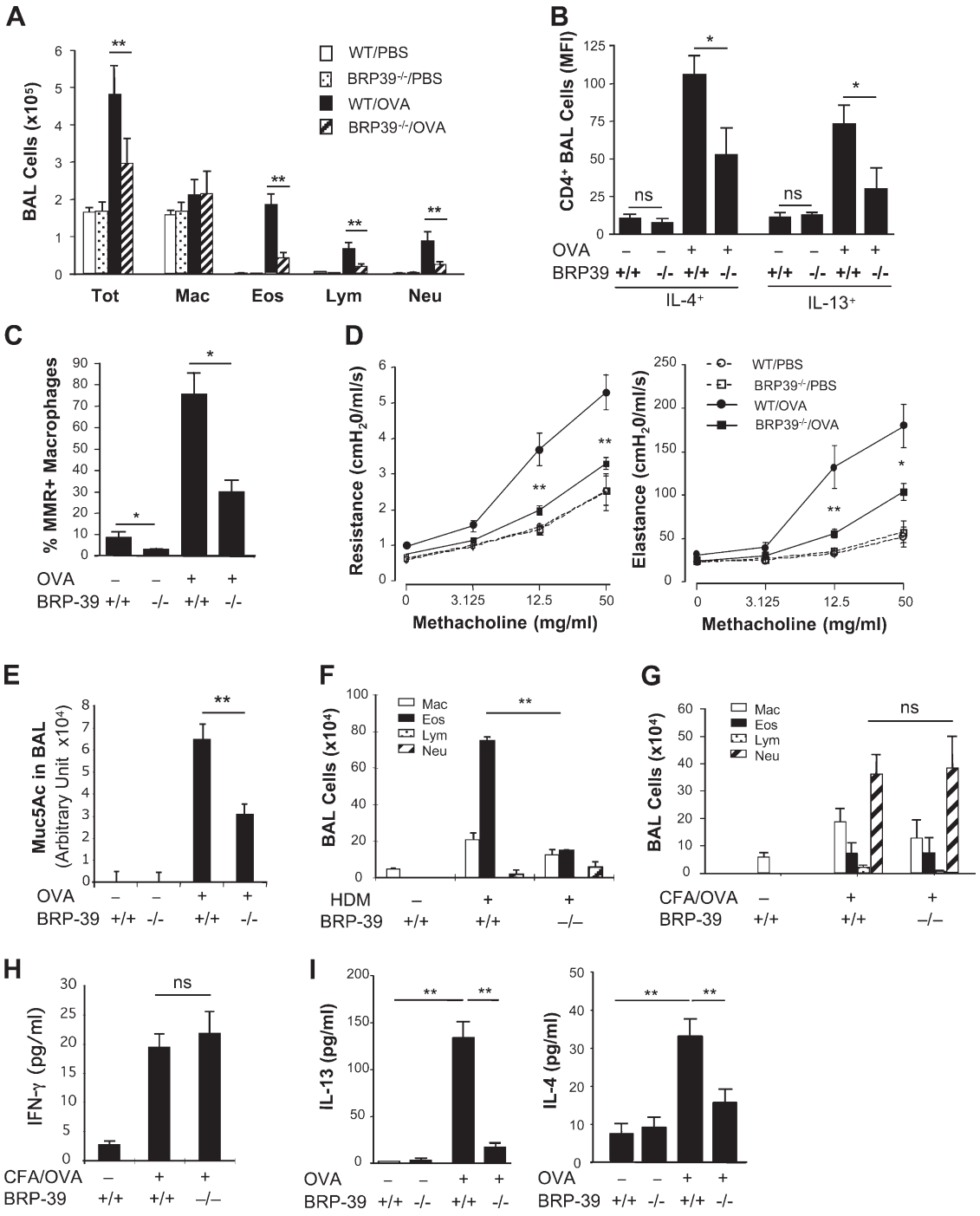

Figure 2. Antigen-induced responses in BRP-39$^{-/-}$ mice. (A–C) BALB/c WT (+/+) and BRP-39$^{-/-}$ mice were sensitized and challenged with OVA (OVA^{+}) or PBS (OVA^{-}). 24 h later, BAL total (Tot) cell, macrophage (Mac), eosinophil (Eos), lymphocyte (Lym), and neutrophil (Neu) recovery were quantitated (A), IL-4– and IL-13–expressing Th2 cells were assessed (B), and MMR expressing alternatively activated macrophages were quantitated (C). (D) AHR was addressed by comparing the airways resistance and elastance of OVA-sensitized and -challenged WT mice (solid circles and solid lines) and BRP-39$^{-/-}$ mice (solid squares and solid lines), WT mice sensitized with OVA and challenged with PBS (circles and dashed lines), and BRP-39$^{-/-}$ mice sensitized with OVA and challenged with PBS (squares and dashed lines). (E) Levels of Muc5ac in the BAL were quantitated by densitometry after slot blotting and immunodetection. (F) WT (+/+) and BRP-39$^{-/-}$ mice were also sensitized and challenged by HDM extract, and BAL cells were evaluated 1 d after the last challenge. (G and H) In evaluations of Th1 responses, WT (+/+) and BRP-39$^{-/-}$ mice were sensitized with CFA/OVA (CFA/OVA^{+}) or PBS (CFA/OVA^{-}) and challenged by OVA. 24 h after the last challenge, BAL cell recovery (G) and BAL IFN-γ levels (H) were evaluated. (I) ELISA evaluations were also used to quantitate the levels of BAL IL-13 and IL-4 in OVA-induced Th2 responses. The values are the mean ± SEM of evaluations in a minimum of five animals and are representative of at least three independent experiments. MFI, median fluorescence intensity; ns, not significant. *, $P < 0.05$; **, $P < 0.01$.

expressed increased levels of CD86, CD80, and CD40 compared with cells from control mice (Fig. 3 E). BRP-39 played an important role in these responses because mDC and pDC accumulation and mDC expression of CD86 and CD40 were significantly decreased in lungs from sensitized and challenged BRP-39$^{-/-}$ mice (Fig. 3, C–E). In contrast, comparable levels of mDC CD80 were seen in the presence and absence of BRP-39 (Fig. 3 E). These studies demonstrate that BRP-39 plays a critical role in the accumulation and activation of pulmonary DC.

BRP-39 in IL-13–induced tissue responses

The studies noted in the previous sections demonstrate that BRP-39 plays a critical role in allergen sensitization. They do not however, rule out the possibility that BRP-39 also plays a critical role in Th2 effector responses. Because IL-13 is the major effector at sites of Th2 inflammation, we addressed this possibility by determining if IL-13 regulates BRP-39 and defining the roles of BRP-39 in the pathogenesis of IL-13–induced inflammation and tissue remodeling. The former studies demonstrated that the levels of BRP-39 mRNA and protein were significantly higher in lungs from IL-13 transgenic (Tg) mice compared with the WT controls (Fig. 4, A and B). This BRP-39 was most prominent in airway epithelial cells and alveolar macrophages (Fig. 4 C). Double-label IHC demonstrated that many of the BRP-39–positive cells were CC10^{+} airway epithelial cells, Pro–surfactant protein C^{+} alveolar type 2 epithelial cells, and CD45^{+} macrophages (Fig. 4 D).

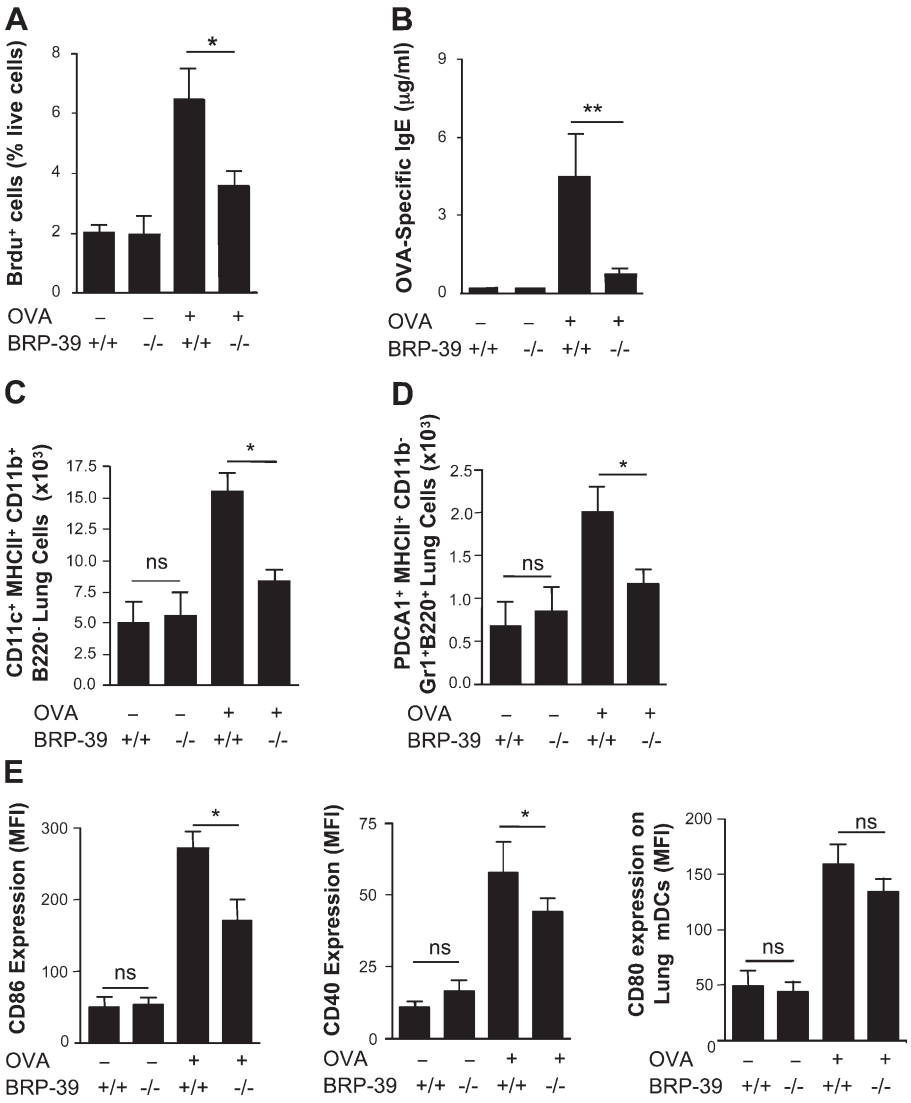

Figure 3. BRP-39 regulation of antigen sensitization. Splenocytes were isolated from the BALB/c WT and BRP-39$^{-/-}$ mice that were sensitized and challenged by PBS (OVA^{-}) or OVA (OVA^{+}). (A and B) After restimulation with OVA, splenocyte proliferation was assessed by BrdU staining (A), and OVA-specific IgE levels (B) were evaluated by ELISA. (C–E) FACS was used to assess mDC (C) and pDC (D) numbers and mDC expression of CD86, CD40, and CD80 (E) in lungs from WT and BRP-39$^{-/-}$ mice that were or were not sensitized and challenged with OVA. The values are the mean ± SEM of evaluations in a minimum of five animals and are representative of three separate experiments. MFI, median fluorescence intensity; ns, not significant. *, $P < 0.05$; **, $P < 0.01$.

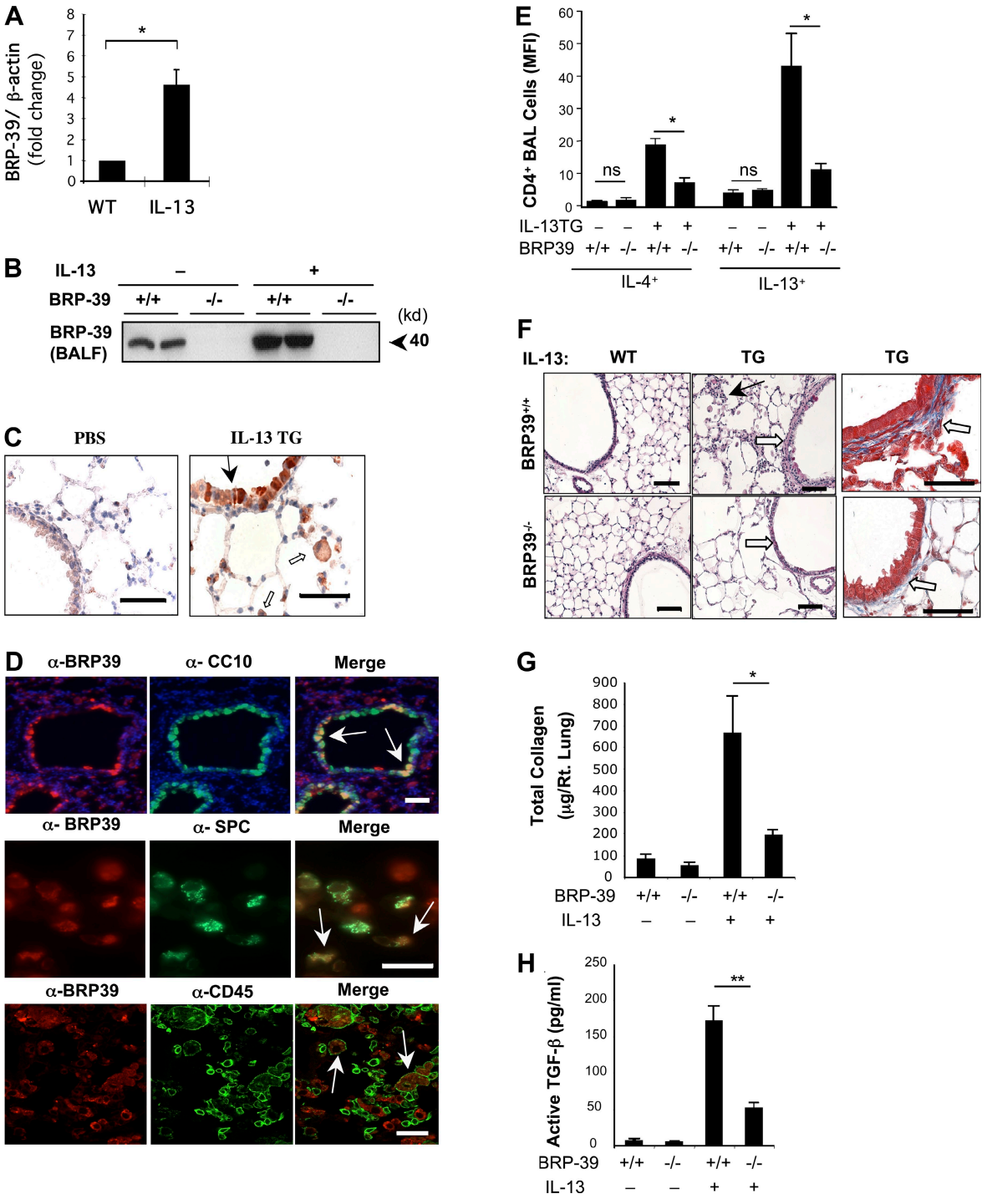

Figure 4. Regulation and roles of BRP-39 in IL-13–induced tissue responses. (A and B) Real-time RT-PCR and Western analysis were used to evaluate the levels of mRNA encoding BRP-39 (A) and BALF BRP-39 protein (B) in lungs from C57BL/6 WT (+/+) and IL-13 Tg mice. (C) The localization of the BRP-39 was evaluated with IHC. Solid arrow, airway epithelium; open arrow, macrophage. (D) Further cellular localization was obtained via double-label IHC using BRP-39 and cell-specific antibodies (CC10, airway epithelial cells; pro-SPC, alveolar type II cells; CD45, leukocytes). Arrows, positive for both antibodies. (E and F) Using WT and IL-13 Tg mice with WT (+/+) and null (−/−) BRP-39 loci, FACS was used to assess BAL CD4+ Th2 cells (E) and histological evaluations were used to evaluate inflammation and airway remodeling (F; left and center are H&E stains [open arrows, peribronchial fibrosis; solid arrow, inflammation] and right are Mallory's trichrome stains [open arrows, subepithelial fibrosis). (G and H) Total collagen content of the right lung and the levels of BAL total TGF-β1 were quantitated by Sircol collagen assay (G) and ELISA (H), respectively. The values in A, E, G, and H are the mean ± SEM of evaluations in a minimum of four animals and are representative of three separate evaluations. B, C, D, and F are illustrative of a minimum of three separate experiments. MFI, median fluorescence intensity. *, $P < 0.05$; **, $P < 0.01$. Bars, 25 μm.

In the latter experiments, IL-13 Tg mice with WT and null BRP-39 loci were generated and the tissue effects of IL-13 in these animals were compared. As previously reported (20, 21), IL-13 caused an eosinophil-, macrophage-, and CD4 Th2 cell–rich inflammatory response and peribronchial fibrosis (Fig. 4, E–G; and not depicted). The BAL and tissue inflammation, CD4 T cell accumulation, and histological and biochemical assessments of tissue fibrosis were significantly decreased in BRP-39$^{-/-}$ mice (Fig. 4 E–G; and not depicted). In accord with our prior demonstration that IL-13 induces airway fibrosis, in part by inducing and activating TGF-β1 (22), the levels of BAL TGF-β1 were also significantly decreased in Tg mice that lacked BRP-39 (Fig. 4 H). Importantly, comparable levels of IL-13 were produced in Tg mice

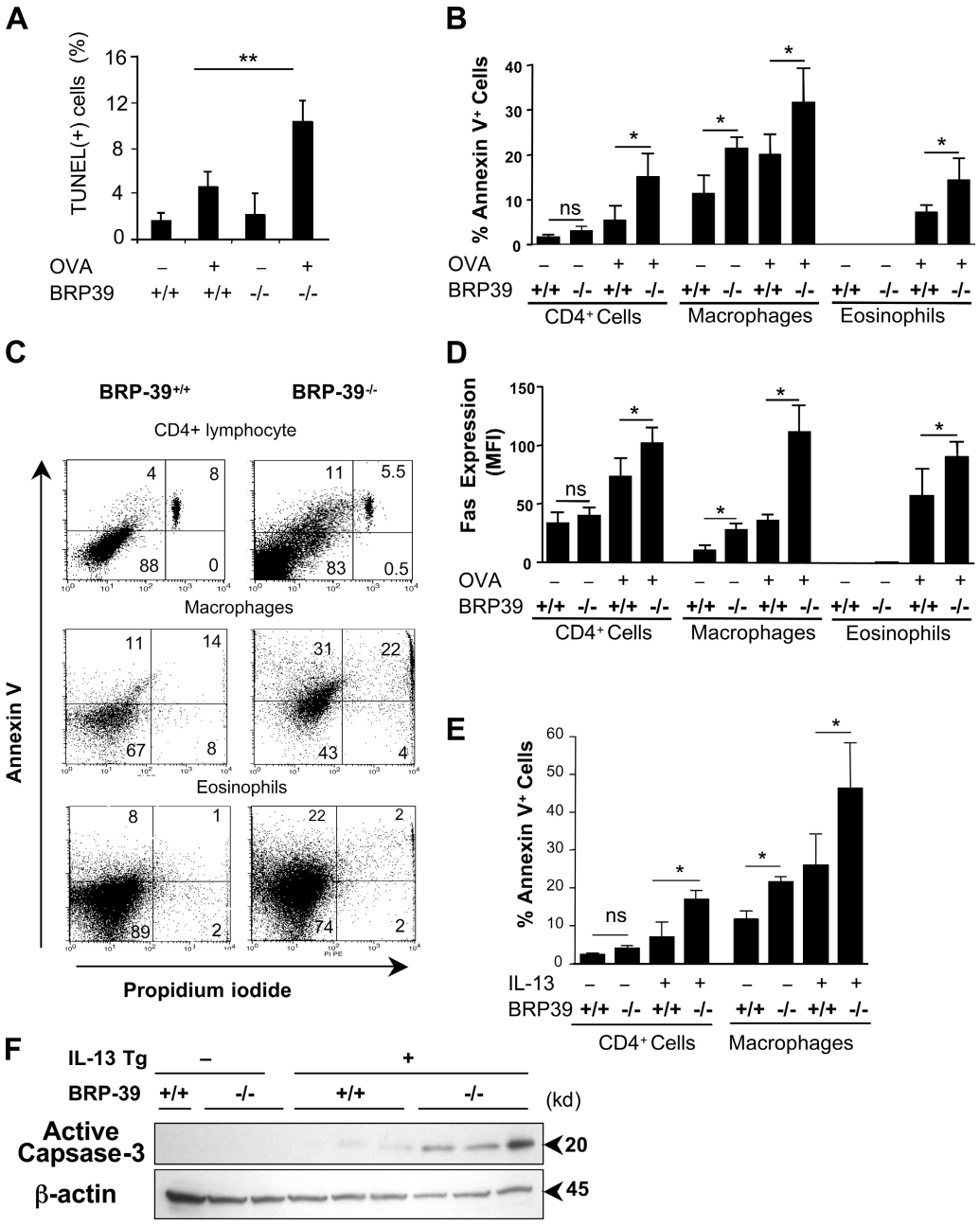

Figure 5. Roles of BRP-39 in inflammatory cell apoptosis/cell death in vivo. BALB/c WT (+/+) and BRP-39$^{-/-}$ mice were sensitized and challenged with OVA (OVA$^+$) or PBS (OVA$^-$). (A–C) Apoptosis was evaluated using TUNEL stains (A) and FACS evaluations to evaluate the expression of annexin V (B), and annexin V and the uptake of PI (C). (D) The expression of Fas was also evaluated by flow cytometry. (E and F) In the C57BL/6 WT and IL-13 Tg mice with WT and null BRP-39 loci, annexin V$^+$ CD4 T cells and macrophages (E) and active caspase 3 expression (F) were evaluated by FACS and Western blot analysis, respectively. The values in A, B, D, and E are the mean ± SEM of evaluations in a minimum of five animals and are representative of at least three separate evaluations. C and F are representative of five and two experiments, respectively. MFI, median fluorescence intensity. *, $P < 0.05$; **, $P < 0.01$.

with WT and null BRP-39 loci (3.2 ± 0.089 ng/ml vs. 3.3 ± 0.074 ng/ml for IL-13 Tg/BRP-39$^{+/+}$ vs. IL-13 Tg/BRP-39$^{-/-}$ mice). These studies demonstrate that BRP-39 is induced by and plays a critical role in the pathogenesis of the IL-13 effector responses that generate inflammation and airway remodeling.

BRP-39 regulation of inflammatory cell apoptosis/cell death

To further understand the mechanisms by which BRP-39 contributes to Th2 effector responses, we next compared the cell death responses of inflammatory cells in OVA-plus-alum–sensitized and –challenged WT and BRP-39$^{-/-}$ mice and IL-13 Tg mice with WT and null BRP-39 loci. The OVA studies revealed enhanced levels of TUNEL and annexin V staining of lung and BAL CD4 cells, macrophages, and eosinophils in BRP-39$^{-/-}$ mice (Fig. 5, A and B; Fig. S4; and not depicted). This included cells with enhanced levels of expression of annexin V only (apoptosis) and cells that stained with annexin V and propidium iodide (PI; advanced apoptosis vs. mixed apoptosis and necrosis; Fig. 5 C). Additional mouse examples can be seen in Fig. S5. This in vivo cell death response was associated with enhanced macrophage, T cell and eosinophil, and Fas (CD95) surface expression (Fig. 5 D). In accordance with the findings with OVA, the blunted inflammatory responses in IL-13 Tg mice that were deficient in BRP-39 were also associated with enhanced TUNEL staining, enhanced levels of CD4 cell and macrophage apoptosis, and enhanced levels of caspase 3 activation (Fig. 5, E and F; and not depicted). These studies demonstrate that BRP-39 is an important inhibitor of eosinophil, T cell, and macrophage death receptor–mediated apoptosis/cell death in vivo.

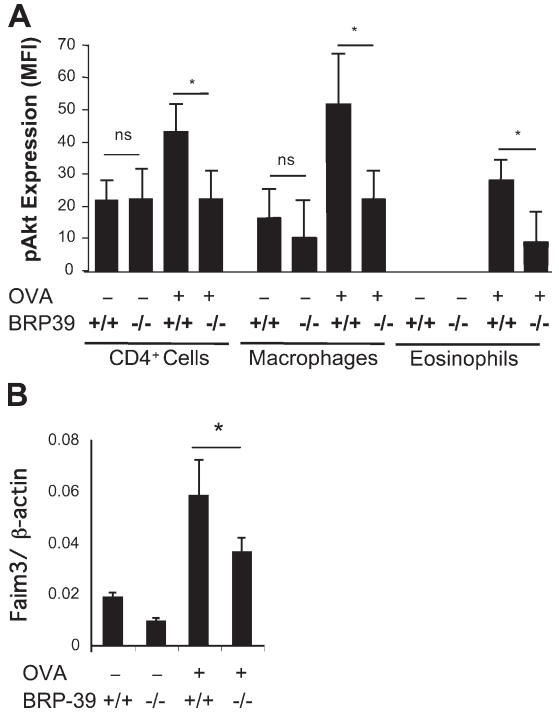

Figure 6. Roles of BRP-39 in AKT phosphorylation and Faim 3 expression. BALB/c WT (+/+) and BRP-39$^{-/-}$ mice were sensitized and challenged with OVA (OVA^{+}) or PBS (OVA^{-}). (A and B) FACS and real-time RT-PCR were used to evaluate the expression of phosphorylated Akt (A) and the levels of mRNA encoding Faim 3 (B), respectively. The values in A and B are the mean ± SEM of evaluations in a minimum of five animals and are representative of at least two separate evaluations. MFI, median fluorescence intensity. *, $P < 0.05$.

BRP-39 regulation of apoptosis-inhibiting pathways in vivo

To shed light on the pathways that BRP-39 uses to control inflammatory cell apoptosis, we evaluated known apoptosis-inhibiting pathways in OVA-plus-alum–sensitized and –challenged WT and BRP-39$^{-/-}$ mice. These studies demonstrated that the decreased levels of apoptosis in WT compared with BRP-39$^{-/-}$ mice were associated with enhanced levels of total and activated protein kinase B (PKB)/AKT (Fig. 6 A and not depicted). Similarly, they were associated with enhanced levels of expression of Fas apoptosis-inhibiting molecule (Faim) 3 (Fig. 6 B).

BRP-39 regulation of inflammatory cell apoptosis in vitro

Studies were next undertaken to determine if BRP-39 directly regulated inflammatory cell apoptosis in vitro and to evaluate the lung specificity of the effects that were seen. In these experiments, we compared the cell death responses in T cells and macrophages from WT and BRP-39$^{-/-}$ mice and evaluated the effects of recombinant (r) BRP-39 in these experimental systems. In the experiments with spleen-derived T cells, the cells from BRP-39$^{-/-}$ mice and WT mice that were cultured with FasL or TNF-α in vitro manifested enhanced levels of apoptosis, caspase 3 activation, and Fas expression compared with untreated WT controls (Fig. 7 A and not depicted). These in vitro cell death responses were significantly ameliorated by incubation with rBRP-39 (Fig. 7 A and not depicted). Interestingly, this effect was most prominent on spleen cells in late-stage apoptosis (Annexin V^{+} PI^{low}) versus splenocytes that were in early apoptosis (Annexin V^{+} PI^{-}; unpublished data). Peritoneal macrophages and alveolar macrophages from BRP-39$^{-/-}$ mice also manifest enhanced levels of annexin V staining, Fas expression, and caspase 3 activation (Fig. 7 B and not depicted). These cell death responses were also ameliorated in a dose-dependent fashion by rBRP-39 (Fig. 7 B and not depicted). Interestingly, in both cases, these BRP-39–induced protective responses were associated with enhanced levels of phosphorylation of the antiapoptotic mediator PKB/AKT (Fig. 7, A and B) and the enhanced expression of the apoptosis inhibitor Faim 3 (not depicted). These studies demonstrate that BRP-39 is a direct inhibitor of eosinophil, T cell, and macrophage death receptor–mediated apoptosis/cell death in vitro. They also demonstrate that the antiapoptotic effects of BRP-39 are not restricted to pulmonary cells and are associated with augmented PKB/AKT phosphorylation and Faim 3 induction.

BRP-39 regulation of alternative macrophage activation

The studies noted in the previous sections demonstrate that the accumulation of alternatively activated macrophages was

decreased at sites of Th2- and IL-13–induced inflammation in BRP-39–deficient mice. To determine if BRP-39 directly contributes to alternative macrophage activation and to evaluate the lung specificity of these effects, peritoneal macrophages and alveolar macrophages were obtained from WT mice and incubated with rBRP-39 or vehicle control. In these experiments, rBRP-39 caused a significant increase in arginase 1 activity and induced the expression of the macrophage mannose receptor (MMR) and MHC class II (Fig. 7 C and Fig. S6). It also induced the production of MDC/CCL22 and thymus- and activation-regulated chemokine (TARC)/CCL17 without altering the production of the M1 marker nitric oxide (Fig. S6 and not depicted). In these experiments many of the effects of rBRP-39 on alternative activation were comparable to the effects of rIL-4 (Fig. 7 C and Fig. S6). These studies demonstrate that BRP-39 is a direct stimulator of alternative macrophage activation and that these effects are not restricted to alveolar cell populations.

Effects of Tg YKL-40

The CC10 promoter, reverse tetracycline transactivator, and tetracycline-controlled transcriptional suppressor were next used to overexpress YKL-40 in the mouse lung (Fig. S7 A). These CC10-rtTA-tTS-YKL-40 Tg mice had an appropriately targeted and inducible transgene (BAL YKL-40, 400–450 ng/ml after 48 h of doxycycline [dox] administration; Fig. S7 B) and

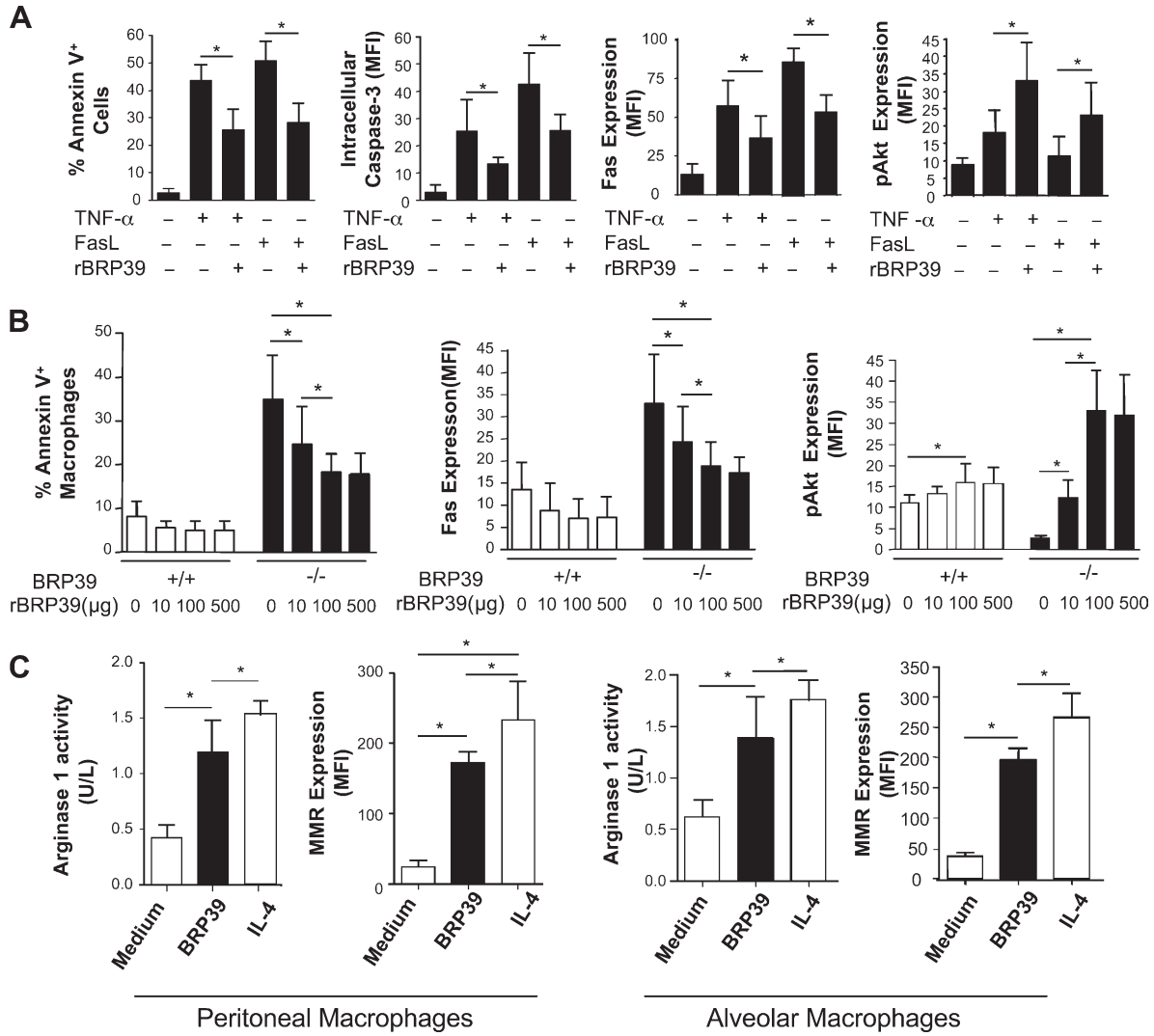

Figure 7. Roles of BRP-39 in splenocyte and macrophage apoptosis/cell death and macrophage activation in vitro. (A) Splenocytes from C57BL/6 WT mice were incubated in the presence or absence of 100 ng/ml TNF-α or 100 ng/ml FasL in the presence or absence of 10 μg/ml rBRP-39. The levels of annexin V staining, intracellular activated caspase 3, Fas expression, and AKT phosphorylation were evaluated. (B) Peritoneal macrophages were elicited from WT (+/+) and BRP-39$^{-/-}$ mice and incubated in the presence or absence of the noted doses of rBRP-39. Annexin V staining, Fas expression, and the levels of phosphorylated AKT were evaluated. *, $P < 0.05$. (C) Peritoneal and alveolar macrophages were obtained from WT mice, incubated with 5 ng/ml rBRP-39 or IL-4 for 48 h, and arginase 1 activity and the expression of MMR were assessed. The values are the mean ± SEM of evaluations in a minimum of five animals and are representative of at least three separate evaluations. MFI, median fluorescence intensity. *, $P < 0.05$.

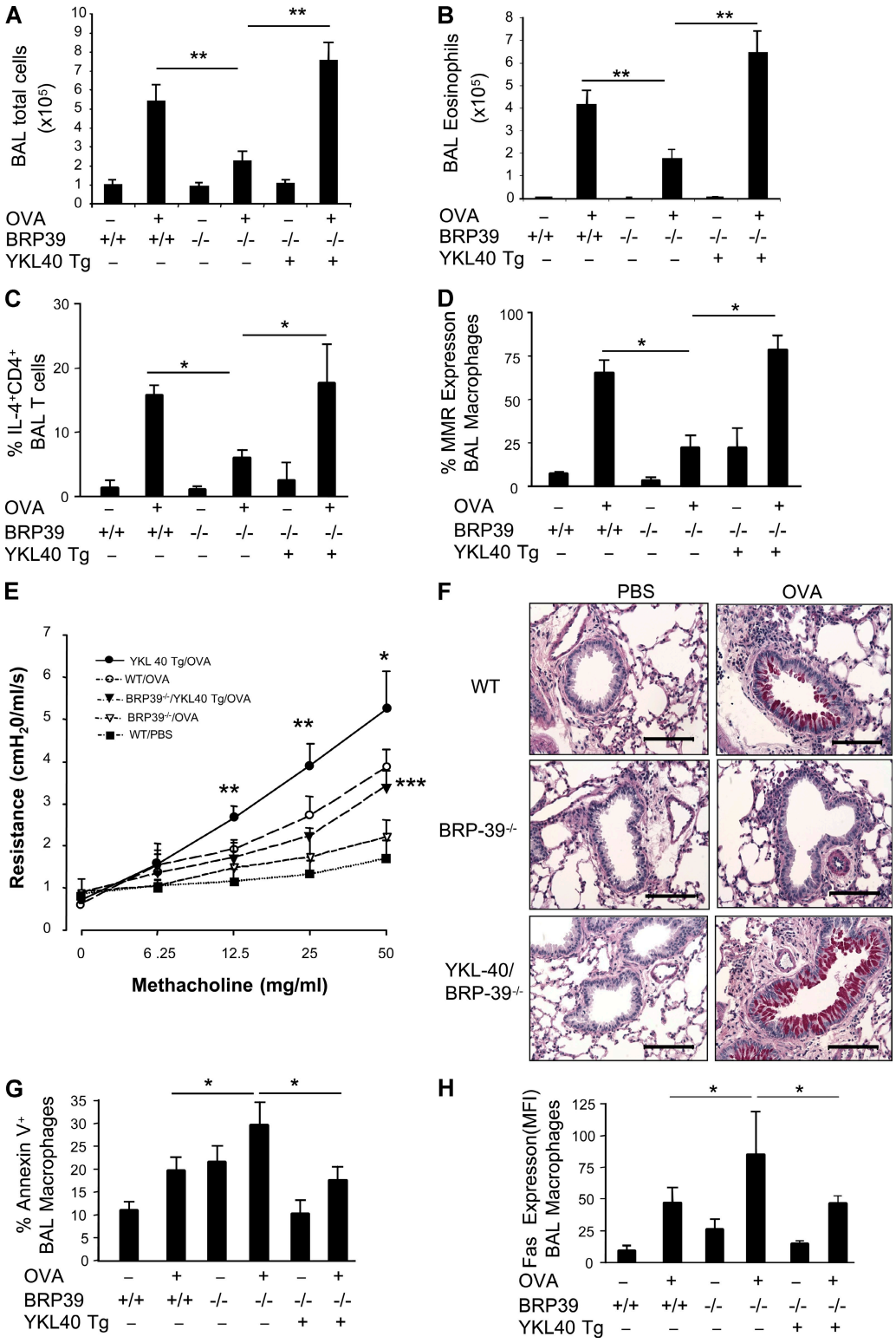

Figure 8. Effects of Tg YKL-40 on OVA-induced Th2 responses in C57BL/6 BRP-39$^{-/-}$ mice. 8-wk-old WT mice, BRP-39$^{-/-}$ mice, and mice that do not make BRP-39 but produce YKL-40 in their lung epithelial cells (BRP-39$^{-/-}$/YKL-40^{+}) were sensitized and challenged as described in Materials and methods. (A–D) Mice were sacrificed 24 h after the last challenge, and BAL total cell (A), eosinophil (B), IL4^{+}CD4^{+} Th2 cells (C), and MMR expression (D) were evaluated. (E) AHR was also addressed by comparing the airway resistance of OVA-sensitized and -challenged WT mice (open circles), BRP-39$^{-/-}$ mice (open squares), YKL40 Tg mice (solid circles), BRP-39$^{-/-}$/YKL-40^{+} mice (solid triangles), and WT mice sensitized with OVA and challenged with PBS (solid squares). *, $P < 0.05$ vs. WT/PBS; **, $P < 0.01$ vs. WT/PBS; ***, $P < 0.01$ vs. BRP-39$^{-/-}$/OVA. (F) Mucus metaplasia was evaluated with D-PAS staining.

normal lungs on gross and light microscopic examination after 4 wk of dox administration (not depicted).

To define the effector functions of our transgene, two approaches were used. In the first, we bred the CC10-rtTA-tTS-YKL-40 mice with the BRP-39$^{-/-}$ mice to generate CC10-rtTA-tTS-YKL-40/BRP-39$^{-/-}$ mice that did not produce BRP-39 and only produced YKL-40 in the epithelium of the lung. This allowed us to define the effects of YKL-40 in the absence of potentially confounding responses induced by endogenously produced BRP-39 and gave us a clear window into the ability of Tg YKL-40 to rescue the defective Th2 response in BRP-39$^{-/-}$ animals. As noted in previous sections, OVA-plus-alum sensitization and OVA challenge caused an impressive eosinophil- and mononuclear cell–rich inflammatory response, increased Th2 cytokine elaboration, increased accumulation of CD4 Th2 cells and alternatively activated macrophages, and increased AHR on methacholine challenge and mucus metaplasia (Fig. 8, A–F; and not depicted). In accordance with these findings, BRP-39 played an important role in the pathogenesis of each of these responses because each was significantly decreased in the BRP-39$^{-/-}$ mice and restored to levels comparable to those in WT animals by epithelial-targeted YKL-40 (Fig. 8, A–F; and not depicted). As also noted, inflammatory cell apoptosis and CD95 expression were increased in OVA-plus-alum–sensitized and OVA-challenged BRP-39$^{-/-}$ mice (Fig. 8, G and H). These responses were also abrogated by CC10 promoter–driven expression of YKL-40 (Fig. 8, G and H).

Experiments were also undertaken with CC10-rtTA-tTS-YKL-40 mice on a WT genetic background. These experiments compared responses in mice with physiological and supraphysiologic levels of BRP-39/YKL-40. At baseline, Tg^{+} mice and WT controls exposed to normal water or dox-treated water for up to 4 wk had similar levels of BAL cell recovery and BAL cell differentials and lungs that could not be differentiated upon histological evaluation (unpublished data). Differences in the methacholine responses of these mice, WT mice, BRP-39$^{-/-}$ mice, and CC10-rtTA-tTS-YKL-40/BRP-39$^{-/-}$ mice were also not noted. (Fig. S8). These YKL-40 Tg mice also had levels of BAL cell recovery and eosinophil recovery that were comparable to those in WT mice after OVA sensitization and challenge (unpublished data). However, dox-treated Tg mice had mildly enhanced levels of alternatively activated macrophages at baseline (Fig. 9 A), modestly enhanced accumulation of alternatively activated macrophages 24 h after OVA sensitization and challenge, and modestly enhanced accumulation of alternatively activated macrophages and Th2 cells 2 wk after OVA sensitization and challenge (Fig. 9, A and B). In addition, the alveolar macrophages and Th2 cells from these mice manifest lower levels of annexin V and Fas expression and higher levels of activated AKT (Fig. 9, C–E). Higher levels of Faim 3 mRNA were also seen in lungs from OVA-sensitized and -challenged YKL-40 Tg mice (Fig. 9 F). In combination, these studies demonstrate that epithelial-targeted YKL-40 rescues the deficient Th2 response in BRP-39$^{-/-}$ mice and regulates alternative macrophage activation, Th2 cell accumulation, inflammatory cell apoptosis, PKB/AKT activation, and Faim 3 expression in the mouse lung.

BRP-39 versus AMCase

The 18-glycosyl-hydolase family contains molecules like BRP-39/YKL-40, which do not degrade chitin, and true chitinases like AMCase. The studies in this manuscript use null mutant, Tg, and in vitro approaches to define the important roles that BRP-39 and YKL-40 play in Th2- and IL-13–induced responses. Prior studies from our laboratory demonstrated that AMCase also plays important roles in these responses (4). To shed light on the biology or these moieties, we compared the regulation and effector profiles of AMCase and BRP-39. In the initial studies, we compared the expression of BRP-39 and AMCase in mice that received in vitro–generated antigen-specific polarized Th1 or Th2 cells, followed by antigen challenge and Tg mice that expressed IL-13 or IFN-γ in the mouse lung. As previously described, AMCase was induced by the Th2 but not the Th1 cells (not depicted) (4). In contrast, BRP-39 was induced by the Th1 and Th2 cells (Fig. 10 A). As noted in this and our prior manuscript (4), IL-13 was a potent stimulator of both 18-glycosyl-hydolase moieties (unpublished data). However, Tg IFN-γ only stimulated BRP-39 (Fig. 10 B and not depicted).

We next compared the regulation and localization of BRP-39 and AMCase in lungs from antigen-challenged mice. In keeping with the observation that IL-13 is a potent stimulator of both moieties, AMCase and BRP-39 were both induced at sites of antigen-driven Th2 inflammation (unpublished data). Interestingly, double-label IHC also demonstrated that both were induced in macrophages and epithelial cells (Fig. 10 C). However, only a subpopulation of these cells expressed both moieties, and the expression of BRP-39 was frequently more prominent than AMCase in the epithelial and macrophage populations (Fig. 10 C).

To gain additional insight into the effector properties of these moieties, we next compared the expression of BRP-39 and AMCase in OVA-sensitized and -challenged and IL-13 Tg mice with WT and null BRP-39 loci. In keeping with our demonstration that AMCase induction is IL-13 dependent and that IL-13 production is decreased in OVA-sensitized and -challenged BRP-39$^{-/-}$ mice, AMCase production was also decreased in BAL fluids from these animals (Fig. 10 D). Interestingly, although IL-13–induced inflammation and remodeling were significantly decreased in the absence of BRP-39,

(G and H) FACS analysis was used to assess alveolar macrophage annexin V^{+} (G) and Fas (H) expression. The values in A–E, G, and H are the mean ± SEM of evaluations in a minimum of five animals and are representative of two separate experiments. F is representative of five similar evaluations. MFI, median fluorescence intensity. *, $P < 0.05$; **, $P < 0.01$. Bars, 50 µm.

AMCase induction was not significantly altered. (Fig. 10 E). These studies demonstrate that IL-13 stimulates BRP-39 and AMCase via different mechanisms. They also demonstrate that the induction of AMCase is not sufficient to overcome the defect in IL-13–induced tissue responses in mice that lack BRP-39. In accord with this finding, BRP-39 was also a potent stimulator of the alternative activation of TARC/CCL17 and MDC/CCL22 production by peritoneal and alveolar macrophages (Fig. S6, Fig. S11, and not depicted). BRP-39 was also a potent activator of mDC (Fig. S6). In contrast, AMCase did not have similar effects on macrophages or DCs (Fig. S6). When viewed in combination, these studies demonstrate that although BRP-39 and AMCase share superficial similarities, they differ in their regulation, sites of production, and effector repertoire.

DISCUSSION

BRP-39 was discovered in mouse breast cancer cells (9). Subsequently, a variety of homologues were described including human YKL-40, human HcGP-39, GP38K (porcine 38-kD heparin-binding glycoprotein), bovine 39-kD whey protein, and *Drosophila melanogaster* imaginal disc growth factors

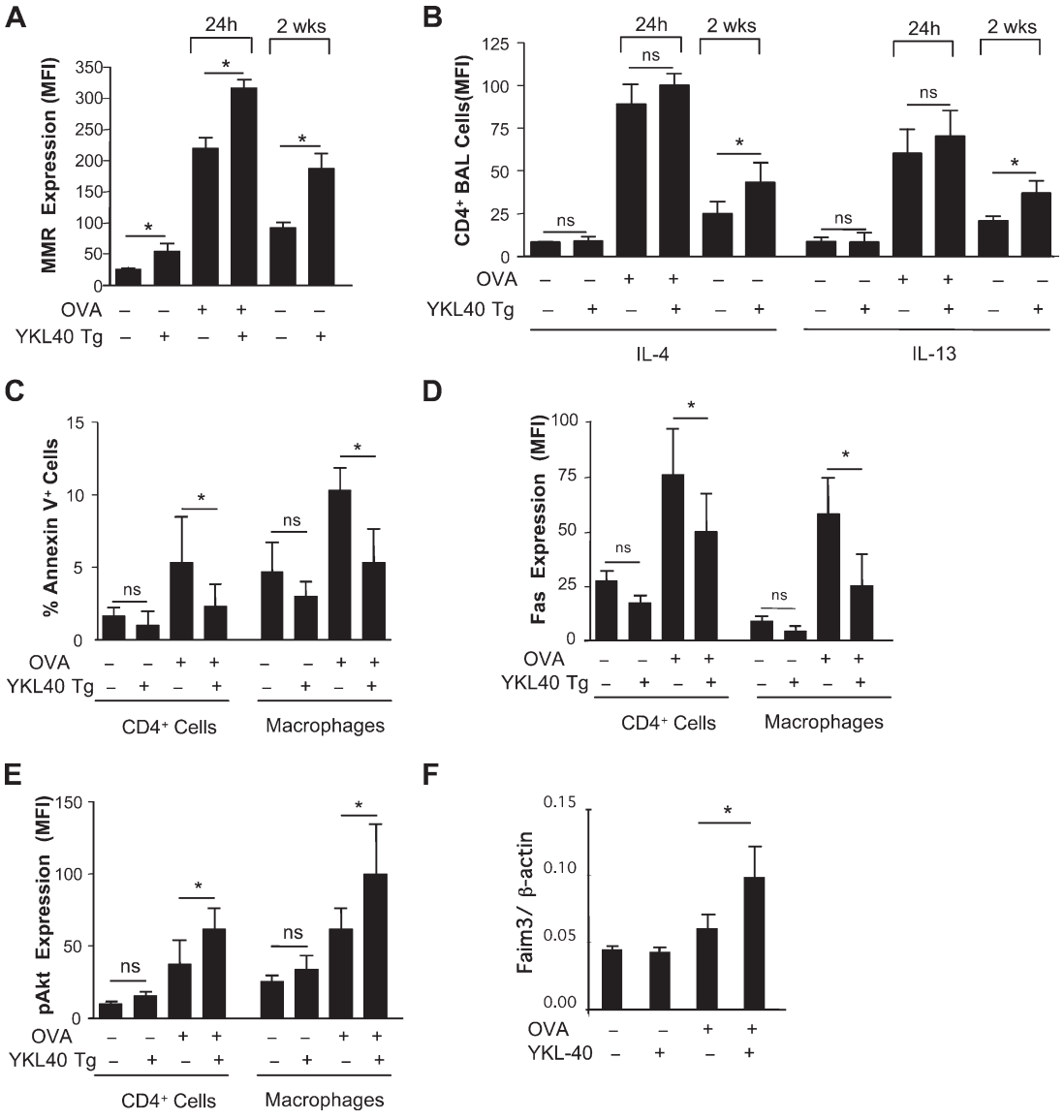

Figure 9. Effects of Tg YKL-40. In A and B, YKL-40 Tg mice (YKL40 Tg+) and Tg negative (−) littermate controls were placed on dox, OVA sensitization and challenge were undertaken, and evaluations were performed 24 h and 2 wk later. (A and B) The levels of MMR expression (A) and the accumulation of IL-4– and IL-13–producing cells (B) in the BAL were evaluated. (C–E) YKL-40 Tg mice (YKL40 Tg+) and Tg negative (−) littermate controls were placed on dox, OVA sensitization and challenge were undertaken, and evaluations were performed 2 wk later. The expression of CD4 cell and macrophage annexin V (C), Fas (D), and the levels of activated Akt (E) were evaluated. *, $P < 0.05$. (F) The levels of Faim 3 mRNA were evaluated 24 h after the last challenge by real-time RT-PCR. The values are the mean ± SEM of evaluations in a minimum of five animals and are representative of two separate experiments. MFI, median fluorescence intensity. *, $P < 0.05$.

(8, 10, 23, 24). In the breast, the expression of BRP-39 is increased during the glandular remodeling that is seen after the cessation of lactation (9). In *Drosophila*, BRP-39–like molecules act as growth factors (23), and in porcine systems, GP38K induces the differentiation of cultured vascular smooth muscle cells (10). Human YKL-40/HcGP-39 is also produced by chondrocytes and synovial cells where it regulates cell proliferation and has mitogenic effects on fibroblasts and synoviocytes (8, 24). This limited body of information suggests that BRP-39/YKL-40 plays a role in tissue remodeling. Because the levels of HcGP-39/YKL-40 are elevated in a variety of human diseases, it has also been thought to contribute to pathological remodeling responses (2, 10, 12, 24–26). Surprisingly, however, the roles of these BRP-39–like moieties in normal physiology and disease pathogenesis are poorly understood. In fact, our limited understanding of the functions of these strongly conserved (and therefore, presumably, biologically important) moieties in mammals and man is believed to be one of the most pressing issues in chitinase/CLP biology (27). To address this issue, we generated and characterized BRP-$39^{-/-}$ mice, YKL-40–overexpressing Tg mice, and mice that were deficient in BRP-39 and expressed YKL-40 selectively in lung epithelial cells. Studies of these mice have added to our understanding of the biology of CLP by demonstrating that BRP-39 plays a critical role in the pathogenesis of Th2 inflammation and IL-13–induced inflammation and remodeling. They also provide insights into the multifaceted mechanisms that underlie these effects by demonstrating that

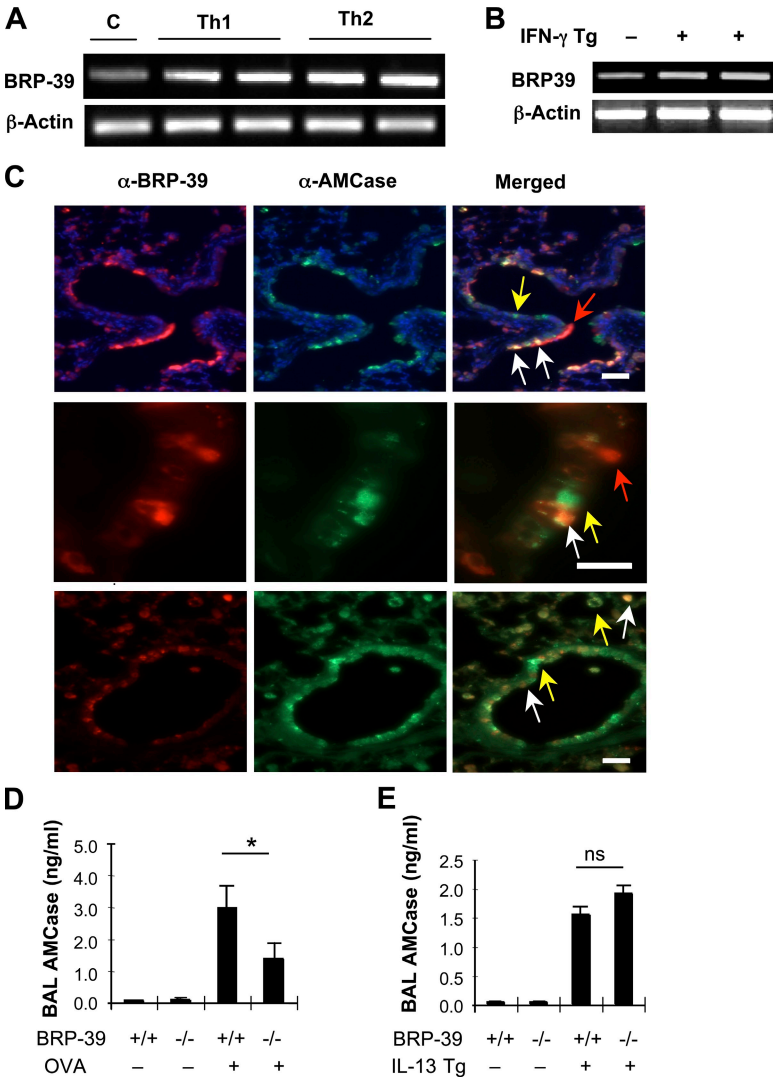

Figure 10. Comparisons of BRP-39 and AMCase. (A) The levels of mRNA encoding BRP-39 in mice that received antigen-specific in vitro–polarized Th1 or Th2 cells and were challenged with antigen (c, control). (B) BRP-39 expression was evaluated by RT-PCR in IFN-γ Tg mice and controls (−). (C) AMCase and BRP-39 expression were localized in the lungs of 2-mo-old IL-13 Tg mice by double-label IHC (white arrows, colocalized; yellow arrows, AMCase; red arrows, BRP-39). (D and E) The levels of BAL AMCase were assessed in OVA-plus-alum–sensitized and OVA-challenged mice (D) and IL-13 Tg mice with WT and null BRP-39 loci (E). The values in D and E are the mean ± SEM of evaluations in a minimum of five animals and are representative of two separate evaluations. *, $P < 0.05$. Bars, 25 µm.

BRP-39 and YKL-40 are important regulators of allergen sensitization and Th2 cytokine effector responses that augment IgE production, DC accumulation and activation, and alternative macrophage activation while inhibiting inflammatory cell apoptosis and CD95 expression and inducing PKB/AKT activation.

We initiated our studies of BRP-39 by comparing the allergen-induced adaptive Th2 responses in WT and BRP-39$^{-/-}$ animals. These studies demonstrated that BRP-39$^{-/-}$ mice do not mount robust antigen-induced Th2 inflammatory reactions. Interestingly, similar defects were seen in experiments with chitin–free and chitin-containing antigens, suggesting that chitin binding does not play an essential role in these reactions. Evaluations of the defective Th2 responses in these mice demonstrated that BRP-39/YKL-40 contributes to Th2 reactions via a variety of mechanisms. First, they demonstrate that BRP-39$^{-/-}$ mice do not sensitize appropriately after antigen exposure when assessed with lymphocyte proliferation assays or assessments of antigen-specific IgE. In accordance with these findings, they demonstrate that BRP-39 is an important stimulator of DC accumulation and activation in this setting. However, our studies also demonstrate that BRP-39–deficient mice also have a significant defect in Th2 cytokine-induced effector responses. This was readily appreciated in the IL-13 Tg mice where, despite producing similar levels of Tg protein, inflammation and fibrosis were diminished in BRP-39–deficient animals. These defective IL-13–induced responses and the diminished antigen-induced responses in BRP-39$^{-/-}$ mice were associated with increased levels of CD4 T cell, macrophage, and eosinophil apoptosis, increased CD95 expression, and diminished levels of CD4 T cell and alternatively activated macrophage accumulation. In vitro studies also demonstrated that rBRP-39 can directly inhibit death receptor–induced T cell and macrophage apoptosis and induce alternative macrophage activation. These observations demonstrate that BRP-39 is an important inhibitor of death receptor–induced inflammatory cell apoptosis and M2 macrophage differentiation. They also suggest that the accelerated cell death responses and diminished M2 differentiation that are seen in BRP-39$^{-/-}$ mice play important roles in the pathogenesis of the defective IL-13 and Th2 responses in these animals. Based on these findings, one can envision how elevated levels of tissue and or circulating BRP-39/YKL-40 can enhance antigen sensitization, increase DC number and activation, inhibit inflammatory cell death, and augment the accumulation of T cells and alternatively activated macrophages, thereby regulating the intensity and natural history of Th2-dominated diseases such as asthma. These findings also provide a potential mechanism, through which YKL-40 can contribute to the severity and activity of diseases in which T cells and macrophages are believed to play important pathogenic roles, such as rheumatoid arthritis, diabetes, inflammatory bowel disease, pulmonary fibrosis, and atherosclerosis.

Many apoptotic signals engage the cell death machinery via the membrane (extrinsic) pathway. This apoptotic mechanism is well documented in T cells, macrophages, and eosinophils (28, 29) and is triggered when ligands like FasL and TNF-α activate surface death receptors such as Fas (CD95). The present studies demonstrate that BRP-39 and YKL-40 inhibit inflammatory cell apoptosis in vivo and in vitro. They also demonstrate that these protective responses are associated with the activation of the well known apoptosis inhibitor PKB/AKT and the more recently described death receptor apoptosis inhibitor Faim 3 (also called TOSO [reference 30]). They also demonstrate that the augmented cell death that is seen in the BRP-39–null mice is associated with the exaggerated expression of CD95 and that rBRP-39 ameliorates FasL- and TNF-α–induced spleen cell death. These observations demonstrate that BRP-39/YKL-40 is an important inhibitor of CD95 expression and death receptor–mediated inflammatory cell apoptosis. They also demonstrate that this protection is associated with and potentially mediated by PKB/AKT and/or Faim 3. This speculation is compatible with the known ability of PKB/AKT and Faim 3 to inhibit Fas-FasL–induced cell death responses and the importance of Fas-mediated inflammatory cell apoptosis in the control of Th2 tissue inflammation (31–34).

Excess tissue fibrosis is a well documented consequence of chronic Th2 inflammatory responses, and IL-13 is believed to be a major mediator of these remodeling reactions (22). The airway fibrosis in the lung-targeted IL-13 Tg mice that were used in these studies is a well appreciated example of this relationship. Previous studies from our laboratory demonstrated that these IL-13–induced fibrotic responses are mediated, in part, by the ability of IL-13 to stimulate TGF-β1 (22). Thus, studies were undertaken to determine if the diminished levels of fibrosis in IL-13 Tg mice that lack BRP-39 are associated with decrements in TGF-β1 induction. These studies provide insight into the mechanisms that BRP-39 may use in this setting by demonstrating that TGF-β1 induction is mediated by a partially BRP-39–dependent mechanism in IL-13 Tg animals. It is important to point out, however, that these studies do not define a role for BRP-39 in the pathogenesis of TGF-β1–induced responses. This possibility will need to be addressed in separate evaluations.

Our studies demonstrate that BRP-39 is produced by macrophages and epithelial cells at sites of Th2 inflammation. However, the importance of BRP-39 in each of these tissue compartments has not been defined. To begin to address this issue, we bred BRP-39$^{-/-}$ mice with YKL-40 Tg mice to obtain mice that were deficient in BRP-39 and produced YKL-40 only in respiratory epithelial cells. We then compared the antigen-induced responses in WT mice, BRP-39–null mice, and CC10-rtTA-tTS-YKL-40/BRP-39$^{-/-}$ animals. These studies demonstrated that the selective expression of YKL-40 in lung epithelial cells is able to fully rescue the defective Th2 response in BRP-39$^{-/-}$ mice. These observations also demonstrated that YKL-40 can effectively crosse species lines and is able to trigger BRP-39 pathways in mouse modeling systems. Additional investigation will be required to define the roles of macrophage BRP-39 in lung biology.

The 18-glycosyl-hydrolase family contains molecules with true chitinase activity, like AMCase, and molecules like BRP-39/YKL-40 that bind to but do not cleave these polysaccharides (1, 27). To date, the majority of the investigations of these moieties have focused on AMCase. These studies have revealed a complex effector profile with AMCase contributing to the pathogenesis of adaptive Th2 inflammation in chitin-free experimental systems (4) and inhibiting type 2 innate immune responses in chitin-driven experimental systems (7). The present studies demonstrate that BRP-39 and YKL-40 also play key roles in the pathogenesis of adaptive Th2 inflammation. Thus, one could be tempted to speculate that AMCase and BRP-39 play similar roles in this and other settings. However, upon deeper analysis it is becoming clear that this assumption is not correct. It is already well documented that these molecules differ in their ability to cleave chitin. Our data also demonstrates that, in contrast to our present understandings regarding AMCase, BRP-399 has similar effects in chitin-free and chitin-containing antigen-driven systems. This finding suggests that the contributions of AMCase in this setting may also be independent of its chitinase enzyme activity. Our studies also demonstrate that BRP-39 and AMCase are regulated differently, are produced by only partially overlapping populations of cells, and differ in their ability to induce alternative macrophage activation and DC activation. In accord with these findings, we noted that although BRP-39 is need to generate Th2 inflammation and AMCase induction in antigen-driven systems, once IL-13 is elaborated it induces AMCase via a BRP-39–independent mechanism. In addition, in the latter setting (the IL-13 Tg mice), AMCase induction was not able to rescue the defect in IL-13–induced inflammation and fibrosis in BRP-39–deficient animals. The literature is filled with examples of multigene families that were initially defined based on sequence or structural homologies and a small number of shared effector properties. However, in most cases, as more knowledge is obtained, differences are appreciated that clarify the unique roles that each family member plays in biology. Our data suggests that we will eventually obtain a similar level of insight into the 18-glycosyl-hydrolase family members and understand more completely the relationship between AMCase and BRP-39. Our demonstration that BRP-39 is a critical mediator in Th2 inflammation that regulates allergen sensitization, inflammatory cell apoptosis, and M2 macrophage differentiation is in keeping with the important roles that M2 macrophages (35, 36), DC activation (37, 38), and inflammatory cell apoptosis (34, 39–41) play in asthma and Th2 inflammatory responses. Additional investigation will be required to determine if these effector responses are generalizable to other members of the 18-glycosyl-hydrolase family and have contributed to the retention of this family in species as diverse as plants and man.

In summary, these studies demonstrate that BRP-39/YKL-40 is induced during and plays a critical role in the pathogenesis of aeroallergen-induced Th2 inflammation and IL-13 effector responses. They also highlight the many ways that BRP-39 and YKL-40 contribute to these responses by describing the novel roles of these molecules in allergen sensitization, IgE induction, Th2 cytokine production, DC activation, and alternative macrophage activation. Lastly, they demonstrate that BRP-39 and YKL-40 are potent inhibitors of death receptor–induced inflammatory cell apoptosis and that these protective responses are associated with the induction and activation of PKB/AKT and the enhanced expression of Faim 3. These studies validate BRP-39/YKL-40 as a therapeutic target against which interventions can be directed to control asthma or other Th2- or macrophage-mediated pathologies.

MATERIALS AND METHODS

Genetically modified mice. C57BL/6 and BALB/c WT mice were obtained from The Jackson Laboratory. Standard targeting approaches and homologous recombination were used to generate BRP-39–null embryonic stem cells and knockout mice (Fig. S1). Mice with null mutations in BRP-39 were generated on a mixed 129/C57BL/6 background and subsequently bred for >10 generations onto a C57BL/6 or BALB/c background. CC10–rtTA–IL-13 Tg mice were generated in our laboratory (20), bred onto a C57BL/6 background, and used in these studies. These mice use the Clara cell 10-kD protein (CC10) promoter and the rtTA (reverse tetracycline transactivator) to target IL-13 to the lung in a dox-inducible manner. Tg mice in which human YKL-40 was tightly and inducibly overexpressed (CC10-rtTA-tTS-YKL-40) in a lung-specific manner were generated using constructs and approaches that have been previously described by our laboratory (Fig. S7) (42). Mice that lacked BRP-39 and produced YKL-40 only in pulmonary epithelial cells (CC10-rtTA-tTS-YKL-40/BRP-39$^{-/-}$) were generated by breeding the CC10-rtTA-tTS-YKL-40 and BRP-39$^{-/-}$ mice. Animal protocols were approved by the Yale University Institutional Animal Care and Use Committee (IACUC), and all experiments were performed according to the guidelines of the Yale University IACUC.

Generation of OVA-induced Th2 responses. To evaluate allergen-induced Th2 responses, OVA sensitization and challenge was accomplished using a modification of the protocols described previously by our laboratory (43). In brief, 6–8-wk-old mice were immunized with 10 μg OVA and 1 mg alum gel (Imject Alum; Thermo Fisher Scientific) on days 1 and 8. Sham-immunized mice received the same amount of saline and 1 mg alum. On days 19–21, the mice received a single 30-min exposure to aerosolized 1% OVA. 1 d after the last challenge, physiological responses were evaluated. At intervals, the mice were sacrificed, BAL was undertaken, and tissue responses were evaluated.

IHC. Single- and double-label IHC were undertaken as previously described by our laboratory (44). These studies used a polyclonal anti–BRP-39 prepared in New Zealand white rabbits with peptides 224–243 of the BRP-39 molecule conjugated with KLH. The specificity of the resulting antiserum was assessed using Western blot and solid-phase binding assays against recombinant mouse AMCase, YM-1, YM-2, BRP-39, oviductin, and chitotriosidase (AstraZeneca) and the purified YM-1/2 protein in the crystals in lungs from IL-13 Tg mice (Fig. S9). Antibodies against pro–surfactant protein C (Millipore), CC10 (Santa Cruz Biotechnology, Inc.), CD45 (BD), and F4/80 (eBioscience) were used to identify alveolar type II cells, airway epithelial cells, and macrophages, respectively. The specificity of the staining was evaluated in experiments in which the primary antiserum was not used and experiments that compared tissue samples from WT and BRP-39$^{-/-}$ animals.

Generation of OVA-induced Th1 responses. To evaluate OVA-induced Th1 response, we used the protocols described previously by Becart et al. (45).

HDM extract sensitization and challenge. HDM sensitization and challenge was accomplished using modifications of the protocols previously described by Zuleger et al. (46).

Histological analysis. The lungs were removed en bloc, inflated at 25-cm pressure with PBS containing 0.5% low melting point agarose gel, fixed in Streck solution (Streck), embedded in paraffin, sectioned, and stained. Hematoxylin and eosin (H&E), and D-PAS or Mallory's trichrome stains were performed in the Research Histology Laboratory of the Department of Pathology at the Yale School of Medicine.

Immunoblot analysis. 50 μg BAL fluids and/or lung lysates were subjected to immunoblot analysis using the polyclonal rabbit antiserum against BRP-39 noted in the IHC section. These samples were fractionated by PAGE, transferred to membranes, and evaluated as described previously by our laboratory (47).

Quantification of BRP-39/YKL-40, AMCase, Th2 cytokines, and TGF-β1. The levels of BRP-39 in BAL or lung lysates were evaluated by ELISA using an anti–BRP-39 rabbit polyclonal IgG for capture and biotinylated anti–BRP-39 followed by horseradish peroxidase–labeled streptavidin (GE Healthcare) for detection. This assay detects as little as 50 pg/ml rBRP-39. YKL-40 was also quantitated by ELISA using the assay provided by MedImmune, Inc. and a commercial assay (Quidel Corporation). The absence of cross reactivity with other chitinase family members (AMCase and chitotriosidase) was confirmed using 100-ng/ml concentrations of purified recombinant proteins. The levels of AMCase were measured using an ELISA (MedImmune, Inc.). The levels of BAL fluid Th2 cytokines and total TGF-β1 (after acid activation) were measured by ELISA using commercial kits (R&D Systems) as directed by the manufacturer.

Assessment of antigen-induced splenocyte proliferation. Mice were sensitized i.p. with OVA in alum on days 1 and 8. On day 19, the mice were killed and the spleens removed. Single cell suspensions were prepared, and splenocytes were cultured in RPMI containing 10% FCS, 5 mM L-glutamine, and 100 U/ml penicillin/streptomycin for 72 h, either with media alone or in the presence of 100 μg/ml OVA. To assess proliferation, BrdU was added to the media according to the manufacturer's protocol (BD). After 72 h, supernatants were removed for cytokine analysis, and proliferation was assessed by staining for BrdU according to the manufacturer's protocol (BD). Samples were read using LSR2 running FACS DIVA software (BD) and further analyzed using FlowJo software (Tree Star, Inc.).

Quantification of OVA-specific IgE. The levels of OVA-specific IgE were measured according to the manufacturer's protocol (MD Biosciences).

Quantification of BAL Muc5ac. The levels of Muc-5ac, a major mouse airway mucin, in BAL fluids were evaluated using slot blotting and immunodetection with anti–Mucin-5AC (45M1; Neo-Markers) as previously described by our laboratory (48).

mRNA analysis. mRNA levels were assessed using real-time RT-PCR as previously described by our laboratories (42, 49). The sequences for the primers that were used were obtained from Primer Bank online (http://pga.mgh.harvard.edu/primerbank).

Flow cytometry. Whole lung cell suspensions were obtained and evaluated using methods previously described by our laboratory (50) and the gating strategy illustrated in Fig. S10.

Assessment of AHR. AHR was determined 24 h after the last OVA challenge (day 22) using previously described methods (51).

Assessments of macrophage activation. Alveolar macrophages and thioglycollate (3%)-elicited peritoneal macrophages were incubated in RPMI 1640 plus 10% FCS for 48 h with or without 10 μg/ml rBRP39, 5 ng/ml IL-4, 10 mg/ml rAMCase, or 1 μg/ml of endotoxin (LPS). Before performing the arginase 1 bioassay (Bioassays Inc.), they were lysed in 0.5% Triton X-100 containing Protease Inhibitor Cocktail tablets (Roche) (52). Surface expression of CD206 and MHC II was evaluated as described by Stein et al. (53). Nitric oxide was evaluated using the standard Griess reaction by adding 50 μl of test solution to 96-well flat-bottomed plates containing 50 μl of Griess reagent (1% sulfanilamide/0.1% N-(1-naphthyl)ethylenediamine dihydrochloride/2.5% H_3PO_4). The production of TARC/CCL17, MDC/CCL22, and IL-12p49 were assessed using commercial ELISA kits (R&D Systems) as described by the manufacturer.

TUNEL staining. DNA fragmentation and cell death were evaluated using TUNEL assays as previously described by our laboratory (42).

Spleen cell apoptosis/cell death evaluations. Harvested spleen cells underwent hemolysis and were resuspended in RPMI 1640 (10% FCS) medium for 24 h. When indicated, 100 ng/ml of mouse rTNF-α (PeproTech), 100 ng/ml of mouse rFasL (PeproTech), and/or 10 μg/ml of mouse rBRP39 (MedImmune, Inc.) were added to the assay. Apoptosis and necrosis were assessed using flow cytometry to assess Annexin V, PI, CD95 (Fas), activated caspase 3, and phospho-Akt as previously described by our laboratory (50).

Quantification of lung collagen. Animals were anesthetized, right heart perfusion was accomplished, and the heart and lungs were removed en bloc. The collagen content of the right lung was determined by quantifying total soluble collagen using the Sircol Collagen Assay kit (Biocolor) according to the manufacturer's instructions.

Passive transfer and activation of polarized Th1 and Th2 cells. Polarized Th1 and Th2 cells were generated in vitro from OTII T cell receptor Tg mice and passively transferred into WT recipients that were then challenged with OVA or vehicle as described previously (54).

Statistics. All data were initially checked for normal/parametric distribution (Kolmogorov-Smirnov test). If parametric distribution was found, analysis of variance was applied to screen for differences among at least three groups. To compare two individual groups, Student's *t* test was applied. If nonparametric distribution was found, the Kruskal-Wallis test was applied to screen for differences among at least three groups, followed by the Mann-Whitney *U* test (Wilcoxon rank-sum test) to compare two individual groups. Statistical analyses were performed using Prism 4.0 (GraphPad Software, Inc.) and STATA (version 8.2 for Windows; StataCorp LP).

Online supplemental material. Fig. S1 illustrates the constructs that were used to generate the BRP-39–null mutant mice. Fig. S2 demonstrates the role of BRP-39 in OVA-induced tissue inflammation. Fig. S3 uses FACS to define the regulation of Th2 cell accumulation by BRP-39. Fig. S4 demonstrates that BRP-39 regulates OVA-induced inflammatory cell apoptosis. Fig. S5 uses FACS to define the role of BRP-39 in OVA-induced inflammatory cell apoptosis. Fig. S6 compares the effects of BRP-39 and AMCase on macrophage and DC activation. Fig. S7 illustrates the constructs that were used to generate the YKL-40 Tg mice and the inducibility of these animals. Fig. S8 illustrates the methacholine responsiveness of the PBS-challenged WT, BRP-$39^{-/-}$, YKL-40 Tg, and BRP-$39^{-/-}$/YKL-40 Tg mice. Fig. S9 shows the specificity of the antisera against BRP-39 and AMCase that were used in this study. Fig. S10 illustrates the gating strategy used in the FACS evaluations. Fig. S11 illustrates the ability of BRP-39 to regulate OVA-induced chemokine production. The supplemental materials and methods include details of the methods that were used for HDM sensitization and challenge, flow cytometry, and the assessments of AHR.

This research was supported by the National Institutes of Health grants RO1-HL-081639 and RO1-HL-064242 to J.A. Elias and RO1-HL-084225 to C.G. Lee. M.H. Sohn is a postdoctoral fellow supported by the Korea Research Foundation Grant (KRF-2008-013-E00032).

The authors have no conflicting financial interests.

Submitted: 10 June 2008
Accepted: 15 April 2009

REFERENCES

1. Boot, R.G., E.F. Blommaart, E. Swart, K. Ghauharali-van der Vlugt, N. Bijl, C. Moe, A. Place, and J.M. Aerts. 2001. Identification of a novel acidic mammalian chitinase distinct from chitotriosidase. *J. Biol. Chem.* 276:6770–6778.
2. Chupp, G.L., C.G. Lee, N. Jarjour, Y.M. Shim, C.T. Holm, S. He, J.D. Dziura, J. Reed, A.J. Coyle, P. Kiener, et al. 2007. A chitinase-like protein in the lung and circulation of patients with severe asthma. *N. Engl. J. Med.* 357:2016–2027.
3. Kawada, M., Y. Hachiya, A. Arihiro, and E. Mizoguchi. 2007. Role of mammalian chitinases in inflammatory conditions. *Keio J. Med.* 56:21–27.
4. Zhu, Z., T. Zheng, R.J. Homer, Y.K. Kim, N.Y. Chen, L. Cohn, Q. Hamid, and J.A. Elias. 2004. Acidic mammalian chitinase in asthmatic Th2 inflammation and IL-13 pathway activation. *Science.* 304:1678–1682.
5. Shahabuddin, M., and D.C. Kaslow. 1994. Plasmodium: parasite chitinase and its role in malaria transmission. *Exp. Parasitol.* 79:85–88.
6. Shahabuddin, M., and J.M. Vinetz. 1999. Chitinases of human parasites and their implications as antiparasitic targets. *In* Chitin and Chitinases. P. Jolles, and R.A.A. Muzzarelli, editors. Birkhauser Verlag, Basel. 223–250.
7. Reese, T.A., H.E. Liang, A.M. Tager, A.D. Luster, N. Van Rooijen, D. Voehringer, and R.M. Locksley. 2007. Chitin induces accumulation in tissue of innate immune cells associated with allergy. *Nature.* 447:92–96.
8. Hakala, B.E., C. White, and A.D. Recklies. 1993. Human cartilage gp-39, a major secretory product of articular chondrocytes and synovial cells, is a mammalian member of a chitinase protein family. *J. Biol. Chem.* 268:25803–25810.
9. Rejman, J.J., and W.L. Hurley. 1988. Isolation and characterization of a novel 39 kDa whey protein from bovine mammary secretions collected during the nonlactating period. *Biochem. Biophys. Res. Commun.* 150:329–334.
10. Shackelton, L.M., D.M. Mann, and J.T. Millis. 1995. Identification of a 38-kDa heparin-binding glycoprotein (gp39k) in differentiating vascular smooth muscle cells as a member of a group of proteins associated with tissue remodeling. *J. Biol. Chem.* 270:13076–13083.
11. Johansen, J.S. 2006. Studies on serum YKL-40 as a biomarker in diseases with inflammation, tissue remodelling, fibroses and cancer. *Dan. Med. Bull.* 53:172–209.
12. Johansen, J.S., P. Christoffersen, S. Moller, P.A. Price, and F. Bendtsen. 2000. Serum YLK-40 is increased in patients with hepatic fibrosis. *J. Hepatol.* 32:911–920.
13. Ostergaard, C., J.S. Johansen, T. Benfield, P.A. Price, and J.D. Lundgren. 2002. YKL-40 is elevated in cerebrospinal fluid from patients with purulent meningitis. *Clin. Diagn. Lab. Immunol.* 9:598–604.
14. Knudsen, L.S., M. Ostergaard, B. Baslund, E. Narvestad, J. Petersen, H.J. Nielsen, B.J. Ejbjerg, M. Szkudlarek, and J.S. Johansen. 2006. Plasma IL-6, plasma VEGF, and serum YKL-40: relationship with disease activity and radiographic progression in rheumatoid arthritis patients treated with infliximab and methotrexate. *Scand. J. Rheumatol.* 35:489–491.
15. Kucur, M., F.K. Isman, B. Karadag, V.A. Vural, and S. Tavsanoglu. 2007. Serum YKL-40 levels in patients with coronary artery disease. *Coron. Artery Dis.* 18:391–396.
16. Rathcke, C.N., and H. Vestergaard. 2006. YKL-40, a new inflammatory marker with relation to insulin resistance and with a role in endothelial dysfunction and atherosclerosis. *Inflamm. Res.* 55:221–227.
17. Ober, C., Z. Tan, Y. Sun, J.D. Possick, L. Pan, R. Nicolae, S. Radford, R.R. Parry, A. Heinzmann, K.A. Deichmann, et al. 2008. Effect of variation in CHI3L1 on serum YKL-40 level, risk of asthma, and lung function. *N. Engl. J. Med.* 358:1682–1691.
18. Johansen, J.S., A.N. Pedersen, M. Schroll, T. Jorgensen, B.K. Pedersen, and H. Bruunsgaard. 2008. High serum YKL-40 level in a cohort of octogenarians is associated with increased risk of all-cause mortality. *Clin. Exp. Immunol.* 151:260–266.
19. Johansen, J.S., B.V. Jensen, A. Roslind, and P.A. Price. 2007. Is YKL-40 a new therapeutic target in cancer? *Expert Opin. Ther. Targets.* 11:219–234.
20. Zheng, T., Z. Zhu, Z. Wang, R.J. Homer, B. Ma, R.J. Riese Jr., H.A. Chapman Jr., S.D. Shapiro, and J.A. Elias. 2000. Inducible targeting of IL-13 to the adult lung causes matrix metalloproteinase- and cathepsin-dependent emphysema. *J. Clin. Invest.* 106:1081–1093.
21. Zhu, Z., R.J. Homer, Z. Wang, Q. Chen, G.P. Geba, J. Wang, Y. Zhang, and J.A. Elias. 1999. Pulmonary expression of interleukin-13 causes inflammation, mucus hypersecretion, subepithelial fibrosis, physiologic abnormalities, and eotaxin production. *J. Clin. Invest.* 103:779–788.
22. Lee, C.G., R.J. Homer, Z. Zhu, S. Lanone, X. Wang, V. Koteliansky, J.M. Shipley, P. Gotwals, P. Noble, Q. Chen, et al. 2001. Interleukin-13 induces tissue fibrosis by selectively stimulating and activating transforming growth factor β_1. *J. Exp. Med.* 194:809–821.
23. Kawamura, K., T. Shibata, O. Saget, D. Peel, and P.J. Bryant. 1999. A new family of growth factors produced by the fat body and active on *Drosophila* imaginal disc cells. *Development.* 126:211–219.
24. Recklies, A.D., C. White, and H. Ling. 2002. The chitinase 3-like protein human cartilage glycoprotein 39 (HC-gp39) stimulates proliferation of human connective-tissue cells and activates both extracellular signal-regulated kinase- and protein kinase B-mediated signalling pathways. *Biochem. J.* 365:119–126.
25. Johansen, J.S., H.S. Jensen, and P.A. Price. 1993. A new biochemical marker for joint injury. Analysis of YKL-40 in serum and synovial fluid. *Br. J. Rheumatol.* 32:949–955.
26. Nordenbaek, C., J.S. Johansen, P. Junker, N. Borregaard, O. Sorensen, and P.A. Price. 1999. YKL-40, a matrix protein of specific granules in neutrophils, is elevated in serum of patients with community-acquired pneumonia requiring hospitalization. *J. Infect. Dis.* 180:1722–1726.
27. Bleau, G., F. Massicotte, Y. Merlen, and C. Boisvert. 1999. Mammalian chitinase-like proteins. *EXS.* 87:211–221.
28. Krammer, P.H., R. Arnold, and I.N. Lavrik. 2007. Life and death in peripheral T cells. *Nat. Rev. Immunol.* 7:532–542.
29. Segal, M., S. Niazi, M.P. Simons, S.A. Galati, and J.G. Zangrilli. 2007. Bid activation during induction of extrinsic and intrinsic apoptosis in eosinophils. *Immunol. Cell Biol.* 85:518–524.
30. Song, Y., and C.O. Jacob. 2005. The mouse cell surface protein TOSO regulates Fas/Fas ligand-induced apoptosis through its binding to Fas-associated death domain. *J. Biol. Chem.* 280:9618–9626.
31. Chuang, Y.H., C.L. Fu, Y.C. Lo, and B.L. Chiang. 2004. Adenovirus expressing Fas ligand gene decreases airway hyper-responsiveness and eosinophilia in a murine model of asthma. *Gene Ther.* 11:1497–1505.
32. Moumen, A., A. Ieraci, S. Patane, C. Sole, J.X. Comella, R. Dono, and F. Maina. 2007. Met signals hepatocyte survival by preventing Fas-triggered FLIP degradation in a PI3k-Akt-dependent manner. *Hepatology.* 45:1210–1217.
33. Su, C.C., Y.P. Lin, Y.J. Cheng, J.Y. Huang, W.J. Chuang, Y.S. Shan, and B.C. Yang. 2007. Phosphatidylinositol 3-kinase/Akt activation by integrin-tumor matrix interaction suppresses Fas-mediated apoptosis in T cells. *J. Immunol.* 179:4589–4597.
34. Wu, W., L. Rinaldi, K.A. Fortner, J.Q. Russell, J. Tschopp, C. Irvin, and R.C. Budd. 2004. Cellular FLIP long form-transgenic mice manifest a Th2 cytokine bias and enhanced allergic airway inflammation. *J. Immunol.* 172:4724–4732.
35. Martinez, F.O., A. Sica, A. Mantovani, and M. Locati. 2008. Macrophage activation and polarization. *Front. Biosci.* 13:453–461.
36. Loke, P., I. Gallagher, M.G. Nair, X. Zang, F. Brombacher, M. Mohrs, J.P. Allison, and J.E. Allen. 2007. Alternative activation is an innate response to injury that requires CD4+ T cells to be sustained during chronic infection. *J. Immunol.* 179:3926–3936.
37. Lambrecht, B.N., M. De Veerman, A.J. Coyle, J.C. Gutierrez-Ramos, K. Thielemans, and R.A. Pauwels. 2000. Myeloid dendritic cells induce Th2 responses to inhaled antigen, leading to eosinophilic airway inflammation. *J. Clin. Invest.* 106:551–559.
38. Lambrecht, B.N., B. Salomon, D. Klatzmann, and R.A. Pauwels. 1998. Dendritic cells are required for the development of chronic eosinophilic airway inflammation in response to inhaled antigen in sensitized mice. *J. Immunol.* 160:4090–4097.
39. Lamb, J.P., A. James, N. Carroll, L. Siena, J. Elliot, and A.M. Vignola. 2005. Reduced apoptosis of memory T-cells in the inner airway wall of mild and severe asthma. *Eur. Respir. J.* 26:265–270.
40. Spinozzi, F., D. de Benedictis, and F.M. de Benedictis. 2008. Apoptosis, airway inflammation and anti-asthma therapy: from immunobiology to clinical application. *Pediatr. Allergy Immunol.* 19:287–295.

41. Vignola, A.M., P. Chanez, G. Chiappara, L. Siena, A. Merendino, C. Reina, R. Gagliardo, M. Profita, J. Bousquet, and G. Bonsignore. 1999. Evaluation of apoptosis of eosinophils, macrophages, and T lymphocytes in mucosal biopsy specimens of patients with asthma and chronic bronchitis. *J. Allergy Clin. Immunol.* 103:563–573.
42. Lee, C.G., S.J. Cho, M.J. Kang, S.P. Chapoval, P.J. Lee, P.W. Noble, T. Yehualaeshet, B. Lu, R.A. Flavell, J. Milbrandt, et al. 2004. Early growth response gene 1–mediated apoptosis is essential for transforming growth factor β_1–induced pulmonary fibrosis. *J. Exp. Med.* 200:377–389.
43. Wang, J., R.J. Homer, L. Hong, L. Cohn, C.G. Lee, S. Jung, and J.A. Elias. 2000. IL-11 selectively inhibits aeroallergen-induced pulmonary eosinophilia and Th2 cytokine production. *J. Immunol.* 165:2222–2231.
44. Homer, R.J., Z. Zhu, L. Cohn, C.G. Lee, W.I. White, S. Chen, and J.A. Elias. 2006. Differential expression of chitinases identify subsets of murine airway epithelial cells in allergic inflammation. *Am. J. Physiol. Lung Cell. Mol. Physiol.* 291:L502–L511.
45. Becart, S., C. Charvet, A.J. Canonigo Balancio, C. De Trez, Y. Tanaka, W. Duan, C. Ware, M. Croft, and A. Altman. 2007. SLAT regulates Th1 and Th2 inflammatory responses by controlling Ca2+/NFAT signaling. *J. Clin. Invest.* 117:2164–2175.
46. Zuleger, C.L., X. Gao, M.S. Burger, Q. Chu, L.G. Payne, and D. Chen. 2005. Peptide induces CD4(+)CD25+ and IL-10+ T cells and protection in airway allergy models. *Vaccine.* 23:3181–3186.
47. Kang, H.R., C.G. Lee, R.J. Homer, and J.A. Elias. 2007. Semaphorin 7A plays a critical role in TGF-β_1–induced pulmonary fibrosis. *J. Exp. Med.* 204:1083–1093.
48. Lee, C.G., R.J. Homer, L. Cohn, H. Link, S. Jung, J.E. Craft, B.S. Graham, T.R. Johnson, and J.A. Elias. 2002. Transgenic overexpression of interleukin (IL)-10 in the lung causes mucus metaplasia, tissue inflammation, and airway remodeling via IL-13-dependent and -independent pathways. *J. Biol. Chem.* 277:35466–35474.
49. Ma, B., M.R. Blackburn, C.G. Lee, R.J. Homer, W. Liu, R.A. Flavell, L. Boyden, R.P. Lifton, C.X. Sun, H.W. Young, and J.A. Elias. 2006. Adenosine metabolism and murine strain-specific IL-4-induced inflammation, emphysema, and fibrosis. *J. Clin. Invest.* 116:1274–1283.
50. Hartl, D., C.H. He, B. Koller, C.A. Da Silva, R. Homer, C.G. Lee, and J.A. Elias. 2008. Acidic mammalian chitinase is secreted via an ADAM17/epidermal growth factor receptor-dependent pathway and stimulates chemokine production by pulmonary epithelial cells. *J. Biol. Chem.* 283:33472–33482.
51. Wagers, S.S., H.C. Haverkamp, J.H. Bates, R.J. Norton, J.A. Thompson-Figueroa, M.J. Sullivan, and C.G. Irvin. 2007. Intrinsic and antigen-induced airway hyperresponsiveness are the result of diverse physiological mechanisms. *J. Appl. Physiol.* 102:221–230.
52. Ochoa, J.B., A.C. Bernard, S.K. Mistry, S.M. Morris Jr., P.L. Figert, M.E. Maley, B.J. Tsuei, B.R. Boulanger, and P.A. Kearney. 2000. Trauma increases extrahepatic arginase activity. *Surgery.* 127:419–426.
53. Stein, M., S. Keshav, N. Harris, and S. Gordon. 1992. Interleukin 4 potently enhances murine macrophage mannose receptor activity: a marker of alternative immunologic macrophage activation. *J. Exp. Med.* 176:287–292.
54. Cohn, L., R.J. Homer, A. Marinov, J. Rankin, and K. Bottomly. 1997. Induction of airway mucus production By T helper 2 (Th2) cells: a critical role for interleukin 4 in cell recruitment but not mucus production. *J. Exp. Med.* 186:1737–1747.